

Subgroup analysis for the functional linear model

Yifan Sun^{a,*}, Ziyi Liu^{a,*}, Wu Wang^{a,**}

^aCenter for Applied Statistics, School of Statistics, Renmin University of China, China

Abstract

Classical functional linear regression models the relationship between a scalar response and a functional covariate, where the coefficient function is assumed to be identical for all subjects. In this paper, the classical model is extended to allow heterogeneous coefficient functions across different subgroups of subjects. The greatest challenge is that the subgroup structure is usually unknown to us. To this end, we develop a penalization-based approach which innovatively applies the penalized fusion technique to simultaneously determine the number and structure of subgroups and coefficient functions within each subgroup. An effective computational algorithm is derived. We also establish the oracle properties and estimation consistency. Extensive numerical simulations demonstrate its superiority compared to several competing methods. The analysis of an air quality dataset leads to interesting findings and improved predictions.

Keywords: ADMM algorithm, B-spline basis, Functional linear regression, Minimax concave penalty, Subgroup analysis

2020 MSC: Primary 62H12, Secondary 62F12

1. Introduction

With the rapid development of information acquisition and transmission technologies, more and more data are being collected continuously during a time interval. Such data are coined as “functional data”. As a new branch of statistics in recent decades, functional data analysis (FDA) encompasses statistical methods and techniques for such data. See [19, 20] for a comprehensive introduction. Functional linear models (FLMs) are useful for modeling the linear relationship between a scalar response and a functional covariate:

$$y_i = \int_{\mathcal{X}} X_i(t)\beta(t)dt + \epsilon_i, i \in \{1, \dots, n\}, \quad (1)$$

where $X_i(t)$ is a square-integrable predictor function defined on a compact support \mathcal{X} of \mathbb{R} , $\beta(t)$ is a square-integrable coefficient function defined on \mathcal{X} , and the random errors ϵ_i are uncorrelated with a zero mean and a constant variance. FLMs have been studied extensively in the literature [5, 6, 11].

In traditional FLMs, the relationship between the response and functional covariate is often assumed to be identical for all subjects. However, due to latent factors or unobserved covariates, the subjects may belong to different subgroups that have heterogeneous relationships between the response of interest and an observed functional covariate. For example, [9] discovered two subgroups of medflies, where the effect patterns of the early fertility process on the lifespan are different across two subgroups. In the study by [18], eighty-four shares quoted at the Paris stock exchange were divided into several subgroups, where the evolution of the index in a past time period has varied effects on the future index for different subgroups. Also, in the empirical analysis conducted in this paper, we find that different regions in China have distinct patterns of association between the NO_2 concentration and average $\text{PM}_{2.5}$ concentration.

*equal contributions from these authors

**Corresponding author. Email address: wu.wang@ruc.edu.cn

For the heterogeneous FLMs, some subgroup analysis approaches have been proposed to identify latent group structures. [18] developed an approach that integrates the partial least squares and functional principal components analysis, but the statistical properties of the proposed approach have not been discussed. Recently, [9] proposed a functional mixture regression (FMR) where the coefficient functions are allowed to vary for different groups of subjects. However, similar to the well-known finite mixture models for traditional linear regressions, FMR also needs to specify a parametric assumption for the conditional density of the scalar responses, often difficult to do in practice.

In addition, the aforementioned subgroup analysis approaches must specify the number of subgroups, which can be problematic in application. Recently, the penalized fusion technique [21] has attracted extensive attention in subgroup analysis [12, 16, 17] and is advantageous in multiple aspects. Specifically, it has a more intuitive definition, determines the number of groups automatically, and can, in principle, accommodate small groups. However, the existing studies focus on linear regression models with scalar covariates, and cannot be directly applied to FLMs.

In this article, we propose a penalized fusion approach for heterogeneous FLMs that can divide the subjects into disjoint subgroups with different coefficient functions. This approach applies a concave penalty to pairwise differences of B-spline coefficient vectors. Compared to FMR, it does not need to specify the number of subgroups in advance; instead, it automatically determines the number of subgroups in a data-driven manner. This, thus, allows us to identify the subgroup structure and estimate coefficient functions simultaneously without any prior knowledge about the subgroup structure.

This work is motivated by the air pollution study in China that focuses on how the average $PM_{2.5}$ relates to NO_2 , and exploring distinctive relationship patterns between $PM_{2.5}$ and NO_2 in different geographical regions, based on the data collected from hundreds of air monitoring stations across China. As a result, we observe a clear spatial clustering that is highly consistent with geographical regionalization of China, where each cluster corresponds to a coefficient function. Moreover, some geographically nonadjacent stations with similar climate characteristics are also combined in the same cluster. Compared with alternative methods, the proposed approach gives a very different subgrouping results, and has a better prediction performance.

To implement the proposed approach, we develop an alternating direction method of multipliers (ADMM) algorithm, which is widely used in penalization-based methods and has desirable convergence properties [4]. Moreover, we establish the consistency property for the proposed approach in identifying the subgroup memberships and estimating the coefficient functions. Specifically, we, firstly, establish the consistency of the oracle estimator with prior knowledge of the true subgroup structure. Then we show that, under mild regularity conditions, the oracle estimator is a local minimizer of the objective function with a high probability. Extensive simulation and real data analysis demonstrate that the proposed approach outperforms several competitors in identifying subgroups and estimating coefficient functions.

The rest of this paper is organized as follows. We propose the heterogeneous functional linear model, introduce a penalized fusion estimation approach along with the ADMM algorithm, and establish theoretical properties in Section 2. In Section 3, we evaluate the finite sample properties of the proposed approach via simulation studies. We use the proposed approach to analyze an air quality dataset in Section 4. Section 5 gives some concluding remarks. The details of the algorithm, proofs of theorems, and additional results of numerical simulations are provided in the supplementary material.

2. Methods

2.1. Penalized fusion estimation

Consider a dataset with n independent samples, each with a scalar response and a functional covariate. For the i th subject, let y_i be the response, and $X_i(\cdot)$ be the functional covariate defined on a compact set $\mathcal{X} = [0, T]$. Assume that the data have been standardized such that there is no intercept. Consider the heterogeneous FLM:

$$y_i = \int_{\mathcal{X}} X_i(t)\beta_i(t)dt + \epsilon_i, i \in \{1, \dots, n\}, \quad (2)$$

where the random errors ϵ_i 's are uncorrelated with mean 0 and variance σ^2 , and $\beta_i(\cdot)$ is the unknown coefficient function defined on \mathcal{X} . Different from the classical FLM, each subject has its own unique coefficient function.

We assume that n subjects form K disjoint subgroups and the coefficient functions are the same within each subgroup. Specifically, let $\mathcal{G} = \{\mathcal{G}_1, \dots, \mathcal{G}_K\}$ be a partition of $\{1, \dots, n\}$, where $K (K \leq n)$ is the number of subgroups. Then $\beta_i = \beta_j$ for any $i, j \in \mathcal{G}_k$. As such, subgroup analysis amounts to determining which β_i 's are equal to each other. To this end, we adopt a penalized fusion approach, which is more flexible than the FMR and some other techniques. For example, the number of subgroups does not need to be assumed a priori, but rather is determined fully data-driven. In addition, it can potentially accommodate smaller subgroups.

Specifically, we first leverage the B-spline basis method to approximate the coefficient function $\beta_i(\cdot)$'s. The q th-order B-spline basis functions with a set of m internal knots $\{\kappa_l | \kappa_{-q+1} = \dots = \kappa_0 < \kappa_1 < \dots < \kappa_{m+1} = \dots = \kappa_{m+q}, \kappa_l = lT/(m+1), l \in \{0, \dots, m+1\}\}$ are defined recursively [2] as

$$B_l^1(t) = \begin{cases} 1 & \kappa_{l-1} \leq x < \kappa_l \\ 0 & \text{otherwise} \end{cases}$$

and

$$B_l^q(t) = \frac{t - \kappa_{l-1}}{\kappa_{q+l-2} - \kappa_{l-1}} B_{l-1}^{q-1}(t) + \frac{\kappa_{q+l-1} - t}{\kappa_{q+l-1} - \kappa_l} B_l^{q-1}(t), \quad l \in \{1, \dots, m+q\},$$

where $t \in [0, 1]$. Let $p = m + q$. Then the coefficient function $\beta_i(t)$ can be approximated through its projection on the B-spline space as

$$\beta_i(t) \approx \sum_{l=1}^p B_l^q(t) \theta_{il} \equiv \mathbf{B} \boldsymbol{\theta}_i,$$

where $\mathbf{B} = (B_1^q(t), \dots, B_p^q(t))$ is a B-spline basis vector, $\boldsymbol{\theta}_i = (\theta_{i1}, \dots, \theta_{ip})^\top = \underset{\boldsymbol{\theta}_i \in \mathbb{R}^p}{\operatorname{argmin}} \|\beta_i - \mathbf{B} \boldsymbol{\theta}_i\|_2$ is a p -dimensional

coefficient vector, and $\|f\|_2 = \sqrt{\int_{\mathcal{X}} f(t)^2 dt}$ as the L_2 norm of a function f . Our goal is to identify the latent subgroup structures of n subjects in terms of coefficient functions β_i 's. This is, thus, equivalent to distinguishing between B-spline coefficient vectors $\boldsymbol{\theta}_i$'s.

Then, we propose the following objective function

$$\begin{aligned} Q_n(\boldsymbol{\theta}; \boldsymbol{\lambda}) = & \frac{1}{2} \sum_{i=1}^n (y_i - \mathbf{H}_i \boldsymbol{\theta}_i)^2 + \frac{1}{2} \lambda_1 \sum_{i=1}^n \|D^2(\mathbf{B} \boldsymbol{\theta}_i)\|_2^2 \\ & + \sum_{i < j} \rho(\boldsymbol{\theta}_i - \boldsymbol{\theta}_j, \omega_{ij} \lambda_2), \end{aligned} \quad (3)$$

where $\boldsymbol{\theta} = (\boldsymbol{\theta}_1^\top, \dots, \boldsymbol{\theta}_n^\top)^\top$, $\mathbf{H}_i = (\int_{\mathcal{X}} X_i(t) B_1(t) dt, \dots, \int_{\mathcal{X}} X_i(t) B_p(t) dt)$, and $\boldsymbol{\lambda} = (\lambda_1, \lambda_2)$ are tuning parameters. In the first penalty term, we denote D^2 as the second-order differential operator. In the second penalty term, we take $\rho(\cdot, \cdot)$ as the minimax concave penalty [MCP, 23], to obtain a nearly unbiased and sparse solution. Specifically, $\rho(\boldsymbol{\theta}_i - \boldsymbol{\theta}_j, \omega_{ij} \lambda_2) = \rho_\tau(\|\boldsymbol{\theta}_i - \boldsymbol{\theta}_j\|_2, \omega_{ij} \lambda_2)$, where $\rho_\tau(t, \gamma) = \gamma \int_0^t (1 - \frac{x}{\gamma})_+ dx$ and ω_{ij} 's are pre-specified weights. Note that the Smoothly Clipped Absolute Deviation Penalty [SCAD, 8] and some other concave penalties are also applicable. We obtain the B-spline coefficient vector estimator $\hat{\boldsymbol{\theta}} = (\hat{\boldsymbol{\theta}}_1^\top, \dots, \hat{\boldsymbol{\theta}}_n^\top)^\top$ by minimizing (3) with respect to $\boldsymbol{\theta}$, and the corresponding coefficient function estimator is $\hat{\beta}_i = \mathbf{B} \hat{\boldsymbol{\theta}}_i$ for $i \in \{1, \dots, n\}$. Subjects i and j belong to the same subgroup if and only if $\hat{\beta}_i = \hat{\beta}_j$. Consequently, the prediction of the i th response is given by $\hat{y}_i = \int_{\mathcal{X}} X_i(t) \hat{\beta}_i(t) dt$. Let $\hat{\mathbf{y}} = (\hat{y}_1, \dots, \hat{y}_n)^\top$.

The objective function takes a penalized fusion form. The first term of the objective function measures the lack of fit. The second term controls the smoothness of the estimated coefficient functions. In particular, we adopt the smooth penalty based on the 2nd-order differential of $\mathbf{B} \boldsymbol{\theta}_i$, i.e., β_i , which is a popular choice in functional data analysis. The third term takes a pairwise fusion form and promotes zero differences of B-spline coefficient vectors and hence grouping. The weights ω_{ij} 's allow flexible strength of penalization. For example, in our real-data analysis in Section 4, we take ω_{ij} as the inverse of the distance between locations i and j to encourage locations with a smaller distance to fall into the same subgroups.

2.2. Computing algorithm and implementations

Let $\mathbf{y} = (y_1, \dots, y_n)^\top$, and $\mathbf{H} = \text{diag}\{\mathbf{H}_1, \dots, \mathbf{H}_n\}$. Some algebra shows that we can rewrite the objective function $Q_n(\boldsymbol{\theta}; \lambda)$ as

$$Q_n(\boldsymbol{\theta}; \lambda) = \frac{1}{2}(\mathbf{y} - \mathbf{H}\boldsymbol{\theta})^\top(\mathbf{y} - \mathbf{H}\boldsymbol{\theta}) + \frac{1}{2}\lambda_1\boldsymbol{\theta}^\top\mathbf{G}\boldsymbol{\theta} + \sum_{i < j} \rho_\tau(\|\boldsymbol{\theta}_i - \boldsymbol{\theta}_j\|_2, \omega_{ij}\lambda_2). \quad (4)$$

Here $\mathbf{G} = \mathbf{I}_n \otimes \mathbf{G}_0$, where \otimes is the Kronecker product, \mathbf{I}_n is the $n \times n$ identity matrix, and \mathbf{G}_0 is the $p \times p$ matrix with element $(\mathbf{G}_0)_{sl} = \int_{\mathcal{X}} B_s''(t)B_l''(t)dt$.

Directly minimizing the objective function (4) is challenging because the penalty function is not separable in $\boldsymbol{\theta}_i$'s. As such, we reparameterize by introducing a new set of parameters $\boldsymbol{\eta}_{ij} = \boldsymbol{\theta}_i - \boldsymbol{\theta}_j$. Hence minimizing (4) is equivalent to the constrained optimization problem:

$$\begin{aligned} \min Q_n(\boldsymbol{\theta}, \boldsymbol{\eta}; \lambda) &\equiv \frac{1}{2}(\mathbf{y} - \mathbf{H}\boldsymbol{\theta})^\top(\mathbf{y} - \mathbf{H}\boldsymbol{\theta}) + \frac{1}{2}\lambda_1\boldsymbol{\theta}^\top\mathbf{G}\boldsymbol{\theta} + \sum_{i < j} \rho_\tau(\|\boldsymbol{\eta}_{ij}\|_2, \omega_{ij}\lambda_2), \\ \text{subject to } &\boldsymbol{\theta}_i - \boldsymbol{\theta}_j - \boldsymbol{\eta}_{ij} = 0, \end{aligned}$$

where $\boldsymbol{\eta} = \{\boldsymbol{\eta}_{ij}^\top, i < j\}^\top$. The augmented Lagrangian function reads as

$$\begin{aligned} L_n(\boldsymbol{\theta}, \boldsymbol{\eta}, \boldsymbol{\zeta}; \lambda) &= \frac{1}{2}(\mathbf{y} - \mathbf{H}\boldsymbol{\theta})^\top(\mathbf{y} - \mathbf{H}\boldsymbol{\theta}) + \frac{1}{2}\lambda_1\boldsymbol{\theta}^\top\mathbf{G}\boldsymbol{\theta} + \sum_{i < j} \rho_\tau(\|\boldsymbol{\eta}_{ij}\|_2, \omega_{ij}\lambda_2) \\ &+ \sum_{i < j} \boldsymbol{\zeta}_{ij}^\top(\boldsymbol{\eta}_{ij} - \boldsymbol{\theta}_i + \boldsymbol{\theta}_j) + \frac{\delta}{2} \sum_{i < j} \|\boldsymbol{\eta}_{ij} - \boldsymbol{\theta}_i + \boldsymbol{\theta}_j\|_2^2, \end{aligned} \quad (5)$$

where $\boldsymbol{\zeta} = \{\boldsymbol{\zeta}_{ij}, i < j\}^\top$ are the Lagrange multipliers and δ is the penalty parameter. We adopt the alternating direction method of multipliers (ADMM) algorithm to compute the estimate of $(\boldsymbol{\theta}, \boldsymbol{\eta}, \boldsymbol{\zeta})$. More details are provided in the supplementary material.

Given the estimate $(\boldsymbol{\theta}^{(s)}, \boldsymbol{\eta}^{(s)}, \boldsymbol{\zeta}^{(s)})$ at the s th iteration, the $(s+1)$ th iteration estimates are

$$\boldsymbol{\theta}^{(s+1)} = (\mathbf{H}^\top\mathbf{H} + \lambda_1\mathbf{G} + \delta\mathbf{A}^\top\mathbf{A})^{-1} \left[\mathbf{H}^\top\mathbf{y} + \delta\mathbf{A}^\top(\boldsymbol{\eta}^{(s)} + \frac{1}{\delta}\boldsymbol{\zeta}^{(s)}) \right], \quad (6)$$

where $\mathbf{A} = \Delta \otimes \mathbf{I}_p$. Here $\Delta = \{(\mathbf{e}_i - \mathbf{e}_j), i < j\}^\top$, with \mathbf{e}_i being the n -dimensional column vector whose i th element is 1 and others are 0, \mathbf{I}_p is a $p \times p$ identity matrix and \otimes is the Kronecker product.

$$\boldsymbol{\eta}_{ij}^{(s+1)} = \begin{cases} \mathbf{u}_{ij}^{(s+1)} & \text{if } \|\mathbf{u}_{ij}^{(s+1)}\|_2 \geq \tau\omega_{ij}\lambda_2, \\ \frac{\tau\delta}{\tau\delta-1} \left(1 - \frac{\lambda_2}{\delta\|\mathbf{u}_{ij}^{(s+1)}\|_2} \right) \mathbf{u}_{ij}^{(s+1)} & \text{if } \|\mathbf{u}_{ij}^{(s+1)}\|_2 < \tau\omega_{ij}\lambda_2, \end{cases} \quad (7)$$

where $\mathbf{u}_{ij}^{(s+1)} = \boldsymbol{\theta}_i^{(s+1)} - \boldsymbol{\theta}_j^{(s+1)} - \frac{\boldsymbol{\zeta}_{ij}^{(s)}}{\delta}$,
and

$$\boldsymbol{\zeta}^{(s+1)} = \boldsymbol{\zeta}^{(s)} + \delta(\mathbf{A}\boldsymbol{\theta}^{(s+1)} - \boldsymbol{\eta}^{(s+1)}). \quad (8)$$

The overall algorithm is summarized in Algorithm 1.

Remark 1. In non-convex optimization, it is important to assign appropriate initial values to obtain a good solution. In the numerical study, we use estimates from a homogeneous functional linear model as the initial $\boldsymbol{\theta}^{(0)}$. Specifically, we assume that all subjects have the same coefficient function, and hence, the same B-spline coefficient vector $\tilde{\boldsymbol{\theta}}$, which is a p -dimensional column vector. We apply the penalized B-spline (without fusion penalization) for all n subjects, and obtain $\tilde{\boldsymbol{\theta}}$ by minimizing the following objective function:

$$(\mathbf{y} - \tilde{\mathbf{H}}\boldsymbol{\theta})^\top(\mathbf{y} - \tilde{\mathbf{H}}\boldsymbol{\theta}) + \lambda_1\boldsymbol{\theta}^\top\mathbf{G}_0\boldsymbol{\theta},$$

where $\tilde{\mathbf{H}} = (\mathbf{H}_1^\top, \dots, \mathbf{H}_n^\top)^\top$, λ_1 is determined by minimizing GCV, which will be explicitly defined in the following. The solution is $\tilde{\boldsymbol{\theta}} = (\tilde{\mathbf{H}}^\top\tilde{\mathbf{H}} + \lambda_1\mathbf{G}_0)^{-1} \tilde{\mathbf{H}}\mathbf{y}$. Then we assign $\boldsymbol{\theta}^{(0)} = \underbrace{(\tilde{\boldsymbol{\theta}}^\top, \dots, \tilde{\boldsymbol{\theta}}^\top)^\top}_n$.

Algorithm 1 ADMM for minimizing (5)

- 1: Initialize $\boldsymbol{\theta}^{(0)}$, $\boldsymbol{\eta}^{(0)} = \mathbf{A}\boldsymbol{\theta}^{(0)}$, and $\boldsymbol{\zeta}^{(0)} = \mathbf{0}$. Set $s = 0$.
 - 2: **repeat**
 - 3: Update $\boldsymbol{\theta}^{(s+1)}$ via (6);
 - 4: Update $\boldsymbol{\eta}^{(s+1)}$ via (7);
 - 5: Update $\boldsymbol{\zeta}^{(s+1)}$ via (8);
 - 6: $s = s + 1$.
 - 7: **until** the convergence criterion is met.
 - 8: **return** the estimates of $\boldsymbol{\theta}$ and $\boldsymbol{\eta}$ at convergence.
-

Remark 2. As the standard ADMM algorithm, we track the progress of the algorithm based on the primal residual $\mathbf{R}^{(s+1)} = \mathbf{A}\boldsymbol{\theta}^{(s+1)} - \boldsymbol{\eta}^{(s+1)}$ and dual residual $\mathbf{D}^{(s+1)} = \delta\mathbf{A}^\top(\boldsymbol{\eta}^{(s+1)} - \boldsymbol{\eta}^{(s)})$. The algorithm is terminated when $\|\mathbf{R}^{(s+1)}\|_2 \leq \epsilon^p$ and $\|\mathbf{D}^{(s+1)}\|_2 \leq \epsilon^d$, where ϵ^p and ϵ^d are some small values according to [4]:

$$\epsilon^p = \sqrt{np}\epsilon^{abs} + \epsilon^{rel}\|\mathbf{A}^\top\boldsymbol{\zeta}^{(s)}\|_2, \quad \epsilon^d = \sqrt{\frac{n(n-1)p}{2}}\epsilon^{abs} + \epsilon^{rel}\max\{\|\mathbf{A}\boldsymbol{\theta}^{(s)}\|_2, \|\boldsymbol{\eta}^{(s)}\|_2\}$$

Here ϵ^{abs} and ϵ^{rel} are pre-specified small constants.

Remark 3. For a sufficient large λ_2 , the MCP penalty can force $\boldsymbol{\eta}_{ij} = 0$. We put subjects i and j into the same subgroup if $\boldsymbol{\eta}_{ij} = 0$. As a result, we have \hat{K} estimated subgroups $\hat{\mathcal{G}}_1, \dots, \hat{\mathcal{G}}_{\hat{K}}$, and let the estimated B-spline coefficient function for the k th subgroup be $\hat{\boldsymbol{\alpha}}_k = \sum_{i \in \hat{\mathcal{G}}_k} \hat{\boldsymbol{\theta}}_i / |\hat{\mathcal{G}}_k|$, where $|\hat{\mathcal{G}}_k|$ is the cardinality of $\hat{\mathcal{G}}_k$.

Tuning procedure. The proposed approach involves two tuning parameters λ_1 and λ_2 , where λ_1 controls the smoothness of the estimated coefficient functions and λ_2 controls the structure of subgroups. To reduce the computational cost, we adopt a two-step procedure [25] instead of a traditional grid search for λ_1 and λ_2 . This approach, firstly, searches for an optimal value of λ_2 while fixing λ_1 at a small value (in our numerical analysis, $\lambda_1 = 0.005$), and then selects λ_1 given the optimal λ_2 from the first step. Following [22] and [16], we choose λ_2 in the first step by minimizing a modified BIC

$$\text{BIC} = \log\left(\frac{\|\mathbf{y} - \hat{\mathbf{y}}\|_2^2}{n}\right) + C_{n,p} \frac{\log(n)}{n} df, \quad (9)$$

where $df = \hat{K}p$ and $C_{n,p} = \log(\log(n+p))$. And in the second step, we determine the optimal λ_1 by minimizing

$$\text{GCV} = \frac{\|\mathbf{y} - \hat{\mathbf{y}}\|_2^2}{(1 - \text{tr}\{\tilde{\mathbf{H}}(\tilde{\mathbf{H}}^\top \tilde{\mathbf{H}} + \lambda_1 \mathbf{G})^+ \tilde{\mathbf{H}}^\top\}/n)^2}, \quad (10)$$

where $(\tilde{\mathbf{H}}^\top \tilde{\mathbf{H}} + \lambda_1 \mathbf{G})^+$ is the Moore-Penrose inverse of $\tilde{\mathbf{H}}^\top \tilde{\mathbf{H}} + \lambda_1 \mathbf{G}$ and $\tilde{\mathbf{H}}$ is a variant version of \mathbf{H} . More precisely, $\tilde{\mathbf{H}} = \text{diag}\{\tilde{\mathbf{H}}_1, \dots, \tilde{\mathbf{H}}_{\hat{K}}\}$, where $\tilde{\mathbf{H}}_i = \{H_i^\top | i \in \mathcal{G}_i\}^\top$. The tuning procedure can be iterated more than one round until satisfactory parameters are found.

Realization To implement the proposed approach, we have developed an R package and made it publicly available at <https://github.com/breakerkun/FLM-clustering>. Also, we have provided a demo for two sample datasets with two and three subgroups, respectively. The proposed approach is computationally affordable. For example, for a simulated dataset with $n = 200$, $q = 4$, $m = 8$, and two subgroups, an overall analysis can be accomplished within 75 seconds using a laptop with 2 Intel(R) Core(TM) i5-8250U CPU @ 1.60 GHz CPU cores and 8G RAM. To speed up the computation, all the ADMM related procedures are coded in C++.

2.3. Statistical properties

We assume that n subjects form K disjoint subgroups. Denote $\mathcal{G} = (\mathcal{G}_1, \dots, \mathcal{G}_K)$ as the subgroup set, and $|\mathcal{G}_{\min}| = \min_{1 \leq k \leq K} |\mathcal{G}_k|$. Let $\boldsymbol{\beta}^0 = (\beta_1^0, \dots, \beta_n^0)^\top$ be the true coefficient functions corresponding to the true subgroup set \mathcal{G} , and $\boldsymbol{\xi}^0 = (\xi_1^0, \dots, \xi_K^0)$ be the distinct values of $\boldsymbol{\beta}^0$. We assume the following conditions:

(C1) The error terms in model (2) are uncorrelated with a mean 0 and a variance $\sigma^2 > 0$.

(C2) For each coefficient function β_i ($i \in \{1, \dots, n\}$), $\beta_i \in C^{q-2}(\mathcal{X})$ is a $(q-2)$ -th order ($q \geq 4$) continuously differentiable function defined on a compact set $\mathcal{X} = [0, T]$.

(C3) $\|X_i\|_2 \leq C_1 < \infty$ for $i \in \{1, \dots, n\}$, where C_1 is a constant.

(C4) $|\mathcal{G}_k| = O(n)$ for $k \in \{1, \dots, K\}$, where $n = \sum_{k=1}^K |\mathcal{G}_k|$.

(C5) The penalty function $\rho(x, \lambda)$ is symmetric, non-decreasing and concave in $[0, \infty)$. It is a constant for $x > a\lambda$ for some constant $a > 0$, and $\rho(0, \lambda) = 0$. $\rho'(x, \lambda)$, the derivative of $\rho(x, \lambda)$, exists and is continuous except for a finite number of x , and $\lambda^{-1}\rho'(0^+, \lambda) = 1$.

Conditions (C1) and (C2) are standard assumptions for nonparametric B-spline smoothing functions [7, 14, 24]. Note that β_i is assumed in $C^{q-2}(\mathcal{X})$ so as to be consistent with the fact that B-splines of order q are $(q-2)$ -th order continuously differentiable. Condition (C3) assumes that the covariate function is bounded. Similar conditions have been considered by [3] and [6] to ensure the identifiability of penalized functional linear model, that is, the existence and unicity of the coefficient functions. Condition (C4) gives the diverge rate of the subgroup size, that is, the subgroup size grows as the sample size increases. Condition (C5) is commonly assumed in a high-dimensional model, and some concave penalties such as MCP and SCAD satisfy it.

If the underlying subgroups $\mathcal{G}_1, \dots, \mathcal{G}_K$ are known, the oracle estimator of B-spline coefficients, denoted as $\hat{\theta}^{\text{or}}$, can be defined as

$$\hat{\theta}^{\text{or}} = \arg \min_{\theta \in \mathcal{M}_{\mathcal{G}}} (\mathbf{y} - \mathbf{H}\theta)^\top (\mathbf{y} - \mathbf{H}\theta) + \lambda_1 \theta^\top \mathbf{G}\theta,$$

where $\mathcal{M}_{\mathcal{G}} = \{\theta \in \mathbb{R}^{np} : \theta_i = \theta_j, \text{ for any } i, j \in \mathcal{G}_k, 1 \leq k \leq K\}$. Then we can obtain the oracle estimator of the coefficient functions by $\hat{\beta}^{\text{or}} = \mathcal{B}\hat{\theta}^{\text{or}}$, where $\mathcal{B} = \mathbf{I}_n \otimes \mathbf{B}$. Note that all the expectations, variance, and probabilities mentioned below are conditional on covariate functions X_1, \dots, X_n , and the symbolic notations of condition are omitted for simplicity.

Theorem 1. Let $\lambda_1 \sim |\mathcal{G}_{\min}|^{-(1-\sigma_0)/2}$ for some $0 < \sigma_0 \leq \frac{3}{5}$, and suppose that the number of knots $m \rightarrow \infty$ as $n \rightarrow \infty$ and $m = o(|\mathcal{G}_{\min}|^{(1+\sigma_0)/4})$. Under Conditions (C1)-(C4), for any subgroup \mathcal{G}_k ($1 \leq k \leq K$) and any $i \in \mathcal{G}_k$, we have

$$\|\hat{\beta}_i^{\text{or}} - \beta_i^0\|_2 = O_p(\phi_{|\mathcal{G}_k|}^{1/2}),$$

where $\phi_{|\mathcal{G}_k|} = m\lambda_1^{-1}|\mathcal{G}_k|^{-1} + m^{-2q} + \lambda_1 m^{4-2q} + \lambda_1$.

Theorem 1 establishes the convergence rate of the oracle estimators of coefficient functions when the true subgroup information is known. Since $|\mathcal{G}_{\min}| = O(n)$ and $m \rightarrow \infty$ as $n \rightarrow \infty$, then $\lambda_1 \rightarrow 0$, $\lambda_1 m^{4-2q} \rightarrow 0$, $m^{-2q} \rightarrow 0$, and $m\lambda_1^{-1}|\mathcal{G}_k|^{-1} \rightarrow 0$ as $n \rightarrow \infty$, and thus $\phi_{|\mathcal{G}_k|} \rightarrow 0$ as $n \rightarrow \infty$. The proof of Theorem 1 is provided in the supplementary material.

Let

$$b = \min_{i \in \mathcal{G}_k, j \in \mathcal{G}_{k'}, k \neq k'} \|\beta_i^0 - \beta_j^0\|_2 = \min_{k \neq k'} \|\xi_k^0 - \xi_{k'}^0\|_2$$

be the minimum distance of the common coefficient functions between two different subgroups. Similar to [16] and [25], the minimum distance b needs to be lower bounded to ensure the model with heterogeneous subgroups is identifiable.

Theorem 2. Suppose the conditions in Theorem 1 and Condition (C5) hold. If $cb > a\lambda_2$ and $\lambda_2 \gg \frac{n^{-(1-\sigma_0)/2} p^4}{|\mathcal{G}_{\min}|}$ for some constant $c > 0$, where σ_0 is given in Theorem 1. Then, there exists a local minimizer $\hat{\theta}$ of the objective function $Q_n(\theta; \lambda)$ such that

$$\Pr(\hat{\theta} = \hat{\theta}^{\text{or}}) \rightarrow 1,$$

and

$$\Pr(\hat{\beta} = \hat{\beta}^{\text{or}}) \rightarrow 1,$$

where $\hat{\beta} = \mathcal{B}\hat{\theta}$, and $\hat{\beta}^{\text{or}} = \mathcal{B}\hat{\theta}^{\text{or}}$.

Theorem 2 shows that the oracle estimator $\hat{\theta}^{\text{or}}$ is a strictly local minimizer $\hat{\theta}$ of the objective function $Q_n(\theta; \lambda)$ with a high probability, and accordingly, the estimator of coefficient functions $\hat{\beta}$ is the oracle estimator of coefficient functions $\hat{\beta}^{\text{or}}$. Let $\hat{\xi}$ be the distinct values of $\hat{\beta}$ and $\hat{\xi}^{\text{or}}$ be the distinct values of $\hat{\beta}^{\text{or}}$. By the oracle property in Theorem

2, we have $\Pr(\hat{\xi} = \xi^{\text{or}}) \rightarrow 1$. Consequently, the true subgroups can be recovered with the estimated common coefficient function for subgroup k given as $\hat{\xi}_k = \hat{\beta}_i^{\text{or}}$ for $i \in \mathcal{G}_k$. This result holds given that $b \gg \frac{n^{-(1-\sigma_0)/2} p^4}{|\mathcal{G}_{\min}|}$. Under Condition (C4), we require $b \gg C^* n^{-\frac{3-\sigma_0}{2}} p^4$ for the constant $0 < C^* < \infty$. That is, the L2-distance of the true coefficient functions between subgroups should not be too small, otherwise, the subgroups can not be recovered. The proof of Theorem 2 is given in the supplementary material. With Theorems 1 and 2, we have established that $\hat{\beta}$ converges to β^0 in probability.

3. Numerical simulation

In this section, we conduct two simulation studies to illustrate the finite-sample performance of the proposed approach. In the first study, we consider two subgroups, and in the second study, there are three subgroups. In our simulation, we let $\mathcal{X} = [0, 1]$ and weights $\omega_{ij} = 1$. We fix the B-spline with order $q = 4$ and the number of knots $m = 8$ for all subjects. Following the suggestion of [25], we fix $\delta = 2$ and $\tau = 1$.

Besides the proposed approach, we also consider the following alternatives for comparison: (i) Oracle approach (referred as "Oracle"), under which the subgrouping structure is known, and a penalized B-spline estimator is adopted to estimate the coefficient function in each subgroup. The objective function of the penalized B-spline is

$$Q_h(\boldsymbol{\theta}; \lambda) = \frac{1}{n} \sum_{i=1}^n (y_i - \mathbf{H}_i \boldsymbol{\theta})^2 + \lambda \|D^2(\mathbf{B}\boldsymbol{\theta})\|_2^2$$

where $\boldsymbol{\theta}$ is the common p -dimensional B-spline coefficient vector for all subjects within the same subgroup. (ii) We consider the finite mixture regression (FIMR) approach of [9], which first treats the heterogeneous coefficient functions β_i 's as p -dimensional vectors $\boldsymbol{\theta}_i$'s, and then applies FIMR to the heterogeneous linear regression model: $y_i = \mathbf{H}_i \boldsymbol{\theta}_i + \epsilon_i$. It is realized by using the R package `flexmix`. (iii) We consider two Kmeans-based clustering methods. First, we consider Response-based clustering (referred to as "Resp"), which first clusters the subjects based on response variables via Kmeans, and then applies a penalized B-spline to each subgroup. Second, we consider Residual-based clustering (referred as "Resi"), which applies penalized B-spline under the homogeneity assumption $y_i = \int_0^1 X_i(t)\beta(t)dt + \epsilon_i$, clusters subjects based on the residuals $y_i - \int_0^1 X_i(t)\hat{\beta}(t)dt$ by using Kmeans, and then applies the penalized B-spline estimator again to each subgroup. The FIMR and two Kmeans-based approaches need to determine the number of subgroups. We set the true number of subgroups as the true value. We note that this is not required with the proposed approach and is often not practical in data analysis. For Resp and Resi approaches, the tuning parameter λ is determined by using a grid search with $\lambda \in \{0.0001, 0.001, 0.005, 0.01, 0.025, 0.05, 0.1, 0.5, 1, 5\}$ and GCV criterion.

To assess the subgrouping performance, we consider two measures, namely the number of identified subgroups (\hat{K}) and the Adjusted Rand Index (ARI), where the Adjusted Rand Index measures the agreement between the structure of the estimated subgroups and that of the true subgroups. To assess the estimation performance, we consider the mean squared error (MSE) of the estimated coefficient functions, which is defined as $\sum_{i=1}^n \int_0^1 (\beta_i(t) - \hat{\beta}_i(t))^2 dt/n$. The results are based on 100 independent runs.

3.1. Example 1: two subgroups

We simulate the heterogeneous data with n samples where $n = 40$ and 200 . The n subjects belong to two subgroups, and two subgroup structures are considered: (a) balanced (referred as "B"), where the two subgroups have the same sizes; and (b) unbalanced (referred as "UB"), where the two subgroups have sizes in a ratio of 1:3. The continuous response y_i for subject i from the k th subgroup is generated by

$$y_i = \int_0^1 X_i(t)\xi_k(t)dt + \epsilon_i, \quad (11)$$

where the error terms ϵ_i are independently generated from the normal distribution with mean 0 and variance 1. Each prediction function $X_i(t)$ is generated as a linear combination of B-spline basis functions. Specifically, $X_i(t) = \sum_{l=1}^{\tilde{p}} a_{il}\tilde{B}_l(t)$, where $\tilde{p} = \tilde{m} + \tilde{q}$ with $\tilde{m} = 15$ and $\tilde{q} = 5$. These a_{il} 's are independently generated from the following

distributions: (1) Norm: $N(2, 1)$ and (2) Unif: $U(0, 4)$. $\xi_k(t)$ represents the coefficient function of the k th subgroup, for which we consider the following two scenarios:

(S1) Nonlinear: $\xi_1(t) = 4 \sin(\pi t) - 1$ and $\xi_2(t) = 10(t - 0.5)^2 - 2$. The distance between two functions in $L^2[0, 1]$ is 3.36,

(S2) Linear: $\xi_1(t) = 3t + 2$ and $\xi_2(t) = 3t - 2$. The distance between two functions in $L^2[0, 1]$ is 4.

Figure 1 and Figure C1 in the supplementary material show the distribution of the number of identified subgroups \hat{K} for Scenarios 1 and 2, respectively. The proposed approach can satisfactorily identify the number of true subgroups for all settings. As n increases, the percentage of correctly determining the number of subgroups becomes larger. Subgrouping and estimation results are summarized in Table 1 for Scenario 1 and Table C1 in the supplementary material for Scenario 2. Since the Oracle approach assumes the true subgroup structure, the proposed approach behaves inferior to the Oracle as expected. But it has significant advantages over the FIMR, Resp and Resi approaches. Consider for example Scenario 1, $n = 40$, balanced structure, and a_{ij} 's are generated from the normal distribution $N(2, 1)$. The proposed approach has (ARI, MSE) equal to (0.960, 1.679), compared to (0.889, 41.156) for the FIMR approach, (0.935, 1.934) for the Resp approach, and (0.861, 2.136) for the Resi approach. We observe that, for 100 independent replicates, FIMR either can accurately recover the subgroup structure with $\text{ARI} > 0.95$, or completely fail with $\text{ARI} \approx 0$, leading to a low average ARI and large standard error of ARI. Meanwhile, once FIMR fails in identifying subgroup structure, a tremendous MSE (100 ~ 400) of the estimated coefficient functions is generated. Note that the true number of subgroups is known as a prior for the FIMR, Resi and Resp approaches, whereas it is unknown for the proposed approach. The values of ARI and MSE increase as n grows for the proposed approach. This supports the estimation consistency established in Theorem 1 and 2. To better visualize the estimation results of the proposed approach, we present estimators of the coefficient functions in Figure 2 for Scenario 1 and in Figure C2 in the supplementary material for Scenario 2. It can be observed that the underlying true coefficient function curves can be recovered well.

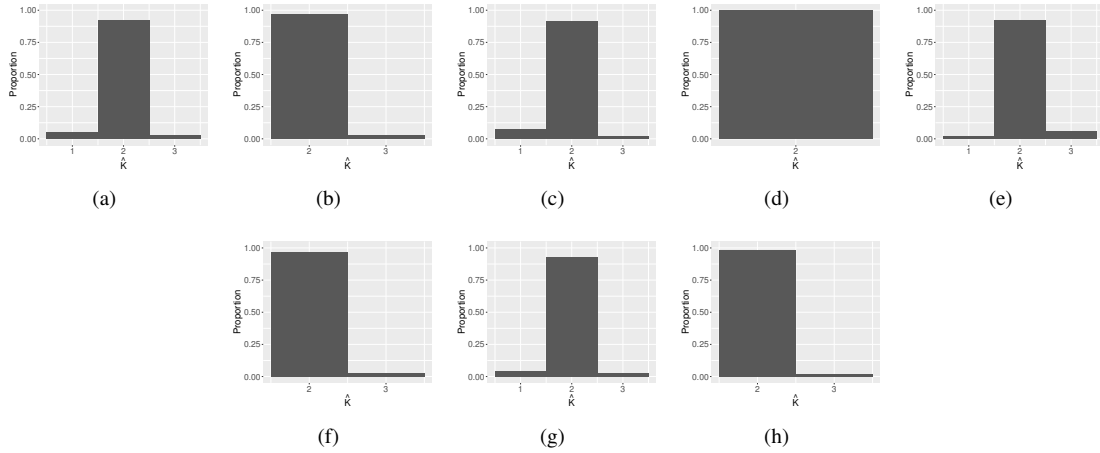


Fig. 1: Simulation results in Example 1: histograms of the estimated number of subgroups \hat{K} by the proposed approach under Scenario 1. (a) and (e) balanced structure with $n = 40$, (b) and (f) balanced structure with $n = 200$, (c) and (g) unbalanced structure with $n = 40$, (d) and (h) unbalanced structure with $n = 200$. (a)-(d) $a_{ij} \sim N(2, 1)$, and (b)-(h) $a_{ij} \sim U(0, 4)$.

Table 1: Simulation results in Example 1: ARI and MSE under Scenario 1. Each cell shows the mean(s.d.).

Structure	a_{il}	Method	$n = 40$		$n = 200$	
			ARI	MSE	ARI	MSE
B	Norm	Proposed	0.960(0.002)	1.679(0.105)	0.993(0.001)	0.392(0.026)
		Oracle		1.348(0.083)		0.327(0.022)
		FIMR	0.889(0.037)	41.156(11.154)	0.933(0.006)	8.217(1.838)
		Resp	0.935(0.007)	1.934(0.187)	0.935(0.005)	0.733(0.039)
		Resi	0.861(0.013)	2.136(0.248)	0.987(0.002)	0.499(0.047)
	Unif	Proposed	0.964(0.005)	1.369(0.121)	0.992(0.002)	0.309(0.014)
		FIMR	0.853(0.045)	42.294(10.365)	0.921(0.008)	6.248(1.530)
		Oracle		1.008(0.089)		0.255(0.016)
		Resp	0.916(0.008)	1.531(0.123)	0.926(0.004)	1.123(0.053)
		Resi	0.845(0.015)	1.703(0.149)	0.987(0.002)	0.408(0.021)
UB	Norm	Proposed	0.954(0.004)	1.337(0.097)	0.981(0.002)	0.477(0.025)
		Oracle		1.187(0.080)		0.353(0.019)
		FIMR	0.908(0.037)	12.426(2.170)	0.975(0.001)	2.094(0.175)
		Resp	0.935(0.005)	1.319(0.139)	0.969(0.002)	0.618(0.035)
		Resi	0.924(0.010)	2.011(0.363)	0.977(0.004)	0.492(0.023)
	Unif	Proposed	0.962(0.004)	1.278(0.136)	0.995(0.001)	0.374(0.029)
		Oracle		1.018(0.085)		0.279(0.014)
		FIMR	0.913(0.041)	9.371(2.794)	0.985(0.002)	3.754(0.159)
		Resp	0.931(0.007)	1.286(0.129)	0.952(0.004)	0.594(0.052)
		Resi	0.927(0.007)	1.493(0.214)	0.969(0.002)	0.476(0.028)

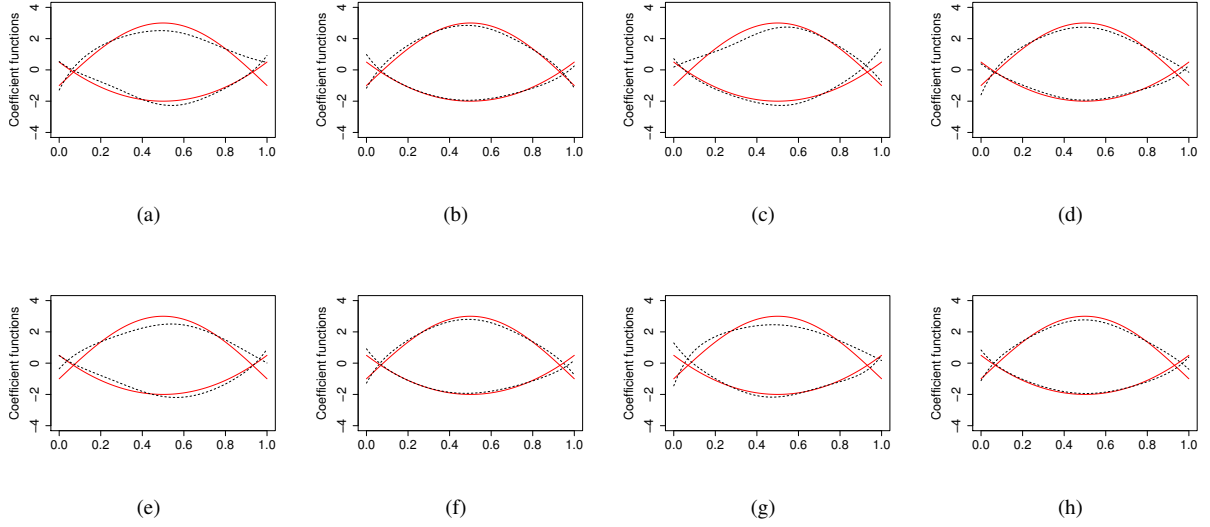


Fig. 2: Simulation results in Example 1: estimation of the coefficient functions by the proposed approach under Scenario 1. (a) and (e) balanced structure with $n = 40$, (b) and (f) balanced structure with $n = 100$, (c) and (g) unbalanced structure with $n = 40$, (d) and (h) unbalanced structure with $n = 200$. (a)-(d) $a_{il} \sim N(2, 1)$, and (b)-(h) $a_{il} \sim U(0, 4)$. Red solid lines represent the true coefficient functions, and black dashed lines represent the estimated coefficient functions.

3.2. Example 2: three subgroups

In this simulation study, we investigate the performance of the proposed approach when there are three subgroups. Let the sample size $n = 60$ and 300 . Under the balanced structure, three subgroups have equal sizes; and under the unbalanced structure, four subgroups have sizes in a ratio of 2:3:5. For the k th subgroup, we simulate data from model (11) with the predictor function and the error terms generated from the same distribution as given in Example 1. The three subgroups have distinct coefficient functions: $\xi_1(t) = -6t + 2$, $\xi_2(t) = 6t^3 + 10t^2 - 10t - 3$, and $\xi_3(t) = -e^{2t} + 3 \sin(2t) + 1.5$, of which the minimum distance (measured in $L^2[0, 1]$) between them is 1.84.

Figure C3 in the supplementary material illustrates the distribution of the estimated number of subgroups by the proposed approach. We obtain similar patterns as those in Figure 1 and Figure C1 in the supplementary material for Example 1. Again, the proposed approach can accurately identify the true number of subgroups. Table C2 in the supplementary material summarizes the results of other statistics. Similar to Example 1, aside from the Oracle approach, the ARI of the proposed approach is always the highest; therefore, it outperforms alternatives in the accuracy of identifying subgroup memberships. In terms of estimation accuracy, the proposed approach is again observed to have favorable performance. Compared to Example 1 where there are only two subgroups, here, the advantages of the proposed approach in terms of subgrouping and estimation are more significant. Consider for example $n = 60$, balanced structure, and a_{il} 's are generated from norm distribution $N(2, 1)$. The proposed approach has (ARI, MSE)=(0.948, 1.969), which is superior to the alternatives: (0.533, 395.569) for the FIMR approach, (0.834, 4.230) for the Resp approach, and (0.781, 7.304) for the Resi approach. FIMR has the worst performance. Figure 3 displays the estimation of coefficient functions by the proposed approach. It can be observed again that the fitting curves produced by the proposed approach are close to the true ones regardless of the simulation settings, indicating that the proposed approach can recover accurately the underlying true coefficient functions. Furthermore, Figure C4 in the supplementary material displays the consumed time (in seconds) running our algorithm with different sample sizes.

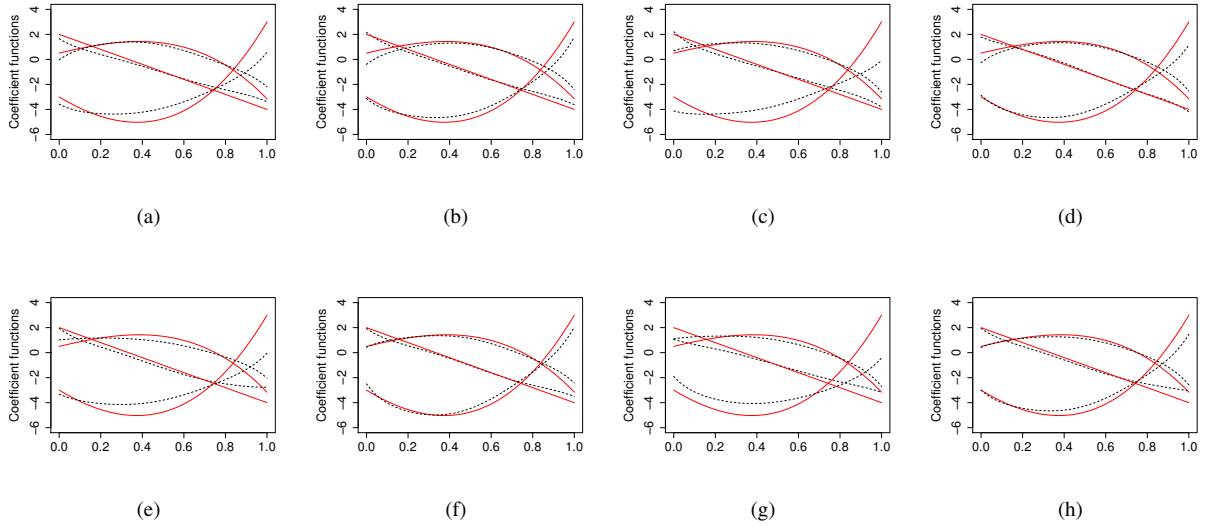


Fig. 3: Simulation results in Example 2: estimation of the coefficient functions by the proposed approach. (a) and (e) balanced structure with $n = 60$, (b) and (f) balanced structure with $n = 300$, (c) and (g) unbalanced structure with $n = 60$, (d) and (h) unbalanced structure with $n = 300$. (a)-(d) $a_{il} \sim N(2, 1)$, and (b)-(h) $a_{il} \sim U(0, 4)$. Red solid lines represent the true coefficient functions, and black dashed lines represent the estimated coefficient functions.

4. Empirical studies

In this section, we apply the proposed approach to China’s air quality data. This data was collected and organized by the World Air Quality Index <http://aqicn.org/>. The concentrations of six major air pollutants, that is, $PM_{2.5}$, PM_{10} , SO_2 , O_3 , NO_2 and CO , are recorded once every eight hours. The dataset consists of 1655 air monitoring stations from February 1, 2015, to January 31, 2016. The response of interest is the average $PM_{2.5}$ concentration during the time period in the study. In the literature, it has been suggested that $PM_{2.5}$ concentration is strongly correlated with NO_2 concentration [1, 13]. In fact, about 50% of total $PM_{2.5}$ in the air is formed from NO_2 and from SO_2 as well. China covers large areas, and these areas have diverse meteorological conditions, population, local industry, traffic, and so on. These differences may lead to distinctive relationship patterns between $PM_{2.5}$ and NO_2 over this huge geographical region. However, most of the existing studies have paid insufficient attention to the potential heterogeneity in the relationship between $PM_{2.5}$ and NO_2 (P-N relationship). As such, we aim to investigate the complex P-N relationship, that is, to explore the underlying subgroups concerning the P-N relationship, and to characterize the relationship pattern for each subgroup.

We focus on the most populated cities in China, which are located in the range of 108° to 135° longitude and 18° to 50° latitude and consist of 25 provinces in Northeast, North, East, Central, and South China. Most of the cities in the area taken into consideration have multiple monitoring stations, and hence, to reduce the computation cost, we randomly select 400 monitoring stations over these large geographical regions. After removing stations that miss more than 50% measurements in NO_2 , a total of 373 stations are included. The closer regions are more likely to possess similar climatic characteristics, meteorological conditions, and industry structure, and thus are more likely to have similar/identical P-N relationships. This “neighborhood effect” can be easily incorporated into our model by setting weights $w_{ij} = 1/d_{ij}$ where d_{ij} is the spherical distance (km) between monitoring stations i and j .

The proposed approach utilizes B-spline with an order $\tilde{q} = 4$ and the number of knots $\tilde{m} = 15$ to approximate the NO_2 concentration (prediction function), and order $q = 4$ and the number of knots $m = 8$ for unknown coefficient functions. The tuning parameters are selected by following the same rule as given in Section 2.2. With the optimal tuning parameters $(\lambda_1^*, \lambda_2^*) = (0.1, 0.6)$, five subgroups are identified, with sizes 102, 121, 51, 52, and 47. Figure 4 (a) displays the grouping results, where monitoring stations within the same subgroup are marked in the same color. We observe a clear spatial clustering that is highly consistent with geographical regionalization of China. The first

subgroup (marked in green) consists of sites in Northeast China, the second subgroup (marked in red) is composed mainly of sites in North China, the third subgroup (marked in orange), the fourth subgroup (marked in purple), and the fifth subgroup (marked in blue) consists of sites in East, Central, and South China, respectively. In addition, our approach successfully combines sites that are geographically nonadjacent yet showing similar P-N relationship into one subgroup. For example, the Northeast (first) subgroup includes sites across three provinces in Northeast China (Heilongjiang, Jilin, and Liaoning) and those in north edge of Jiaodong Peninsular. The Jiaodong Peninsular is offshore across from the Liaodong peninsula which is located south of Liaoning province, and both have temperate oceanity monsoon climate. The estimated coefficient functions of all subgroups are displayed in Figure 4 (b). Overall, the five subgroups have significantly different coefficient functions.

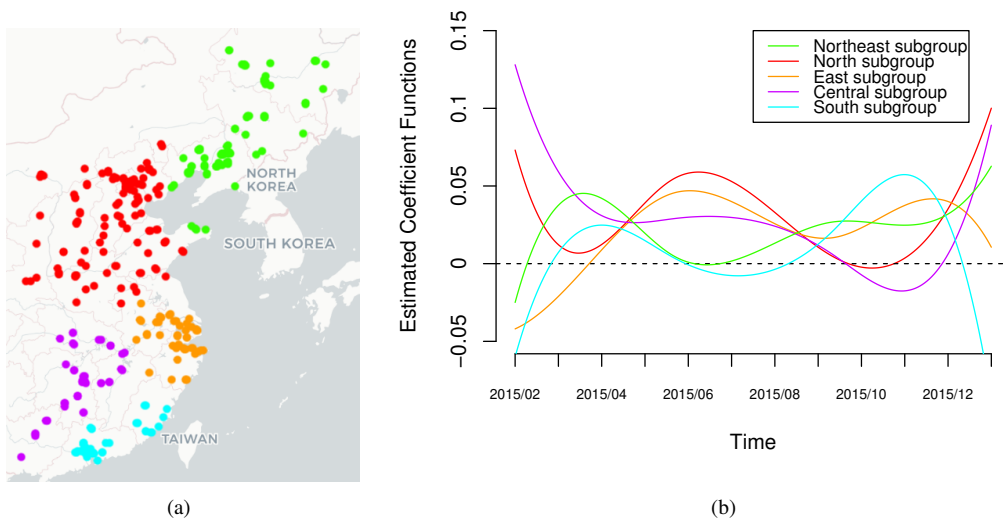


Fig. 4: Data analysis: (a) geographical distribution and (b) estimated coefficient functions of five subgroups. Each color represents a different subgroup.

Data are also analyzed using alternative methods: FIMR, Resi, and Resp. To make different approaches comparable, we fix the number of subgroups in the alternatives to the same as that of the proposed approach. We compute the Normalized Mutual Information (NMI) to measure the similarity between the subgrouping results, with range $[0, 1]$ and a larger value indicating a higher degree of similarity. The results are provided in Table C3 in the supplementary material. We find that the proposed approach has low similarity with the alternatives. As has been noted in many published studies, it is difficult to objectively assess which set of subgroup analysis results are more sensible. As such, we evaluate prediction performance, which may provide support to a certain extent. Specifically, 95%, 90%, 85%, and 80% of the sites are randomly selected as the training data, and the remaining sites are served as the testing data. Estimation is conducted using the training set, and prediction is made with the testing set. The process is repeated independently 50 times. Besides the aforementioned alternatives, we also apply the homogeneous FLM (Homo) to this data. Figure 5 presents the prediction mean square error (MSE). It can be observed that the proposed approach outperforms the alternatives in prediction.

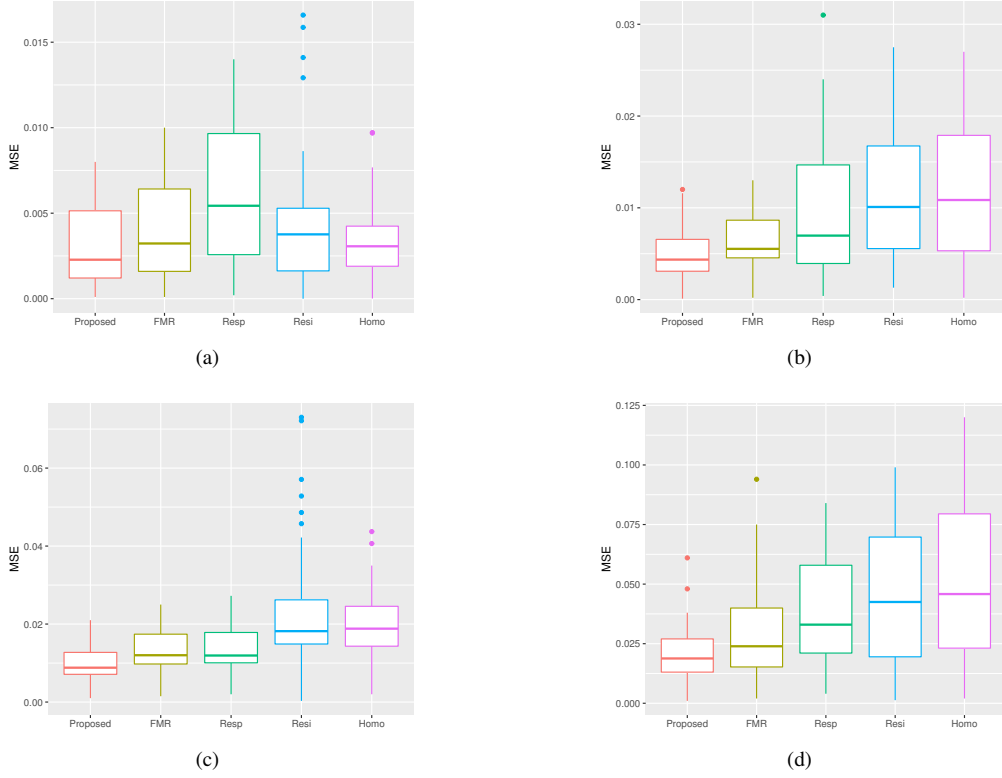


Fig. 5: Prediction mean square errors on test sets which accounts for (a) 5%, (b) 10%, (c) 15%, and (d) 20% of data.

5. Conclusion

In this paper, we developed a fusion penalized approach to conduct a subgroup analysis for the heterogeneous FLM where the responses are scalars and the covariates are functions. The proposed approach can identify the subgrouping structure and estimate the heterogeneous coefficient functions simultaneously and automatically. We adopted the B-spline method to approximate the unknown coefficient functions and applied additional penalization to smooth the estimated coefficient functions. In addition, we grouped subjects by penalizing pairwise differences of B-spline coefficient vectors. We presented the theoretical properties of the proposed approach to ensure its estimation consistency. We implemented an ADMM-based iterative algorithm for numerical computation. The simulation demonstrated favorable performance. In the analysis of air quality data, findings different from those of the alternatives were generated, and an improved prediction was observed.

The proposed approach involves two tuning parameters. How to select viable tuning parameters, and in particular, the impact of heterogeneity on standard tuning parameter procedure, warrant further investigation. The proposed approach can be naturally extended to the FLM with multiple predictor functions. Beyond the FLM considered in this article, there are many other types of responses/models for functional data. It will be of interest to extend the proposed analysis to other responses/models.

Acknowledgements

This research was supported by the National Natural Science Foundation of China (grants 12171479), and the Fund for building world-class universities (disciplines) of the Renmin University of China (Project No. KYGJC2022007). The computer resources were provided by the Public Computing Cloud Platform of the Renmin University of China.

Appendix

This supplementary material contains the details of ADMM algorithm and the proof of Theorem 1 and 2 in the main manuscript, as well as additional figures and tables in the experiments.

A. Details of ADMM algorithm

For a given $(\boldsymbol{\eta}, \boldsymbol{\zeta})$, the component of the Lagrange function L_n that depends on $\boldsymbol{\theta}$ is

$$\mathcal{L}_n(\boldsymbol{\theta}; \boldsymbol{\lambda}) = \frac{1}{2}(\mathbf{y} - \mathbf{H}\boldsymbol{\theta})^\top (\mathbf{y} - \mathbf{H}\boldsymbol{\theta}) + \frac{1}{2}\lambda_1 \boldsymbol{\theta}^\top \mathbf{G}\boldsymbol{\theta} + \frac{\delta}{2} \sum_{i < j} \|\boldsymbol{\theta}_i - \boldsymbol{\theta}_j - \boldsymbol{\eta}_{ij} - \frac{1}{\delta} \boldsymbol{\zeta}_{ij}\|_2^2.$$

Introduce $\boldsymbol{\Delta} = \{(\mathbf{e}_i - \mathbf{e}_j), i < j\}^\top$ with \mathbf{e}_i being a n -dimensional column vector whose i th element equals 1 and the rest are equal to 0, and $\mathbf{A} = \boldsymbol{\Delta} \otimes \mathbf{I}_p$ where \mathbf{I}_p is a $p \times p$ identity matrix and \otimes is the Kronecker product. Then the expression of $\mathcal{L}_n(\boldsymbol{\theta}; \boldsymbol{\lambda})$ can be rewritten in a more compact form:

$$\mathcal{L}_n(\boldsymbol{\theta}; \boldsymbol{\lambda}) = \frac{1}{2}(\mathbf{y} - \mathbf{H}\boldsymbol{\theta})^\top (\mathbf{y} - \mathbf{H}\boldsymbol{\theta}) + \frac{1}{2}\lambda_1 \boldsymbol{\theta}^\top \mathbf{G}\boldsymbol{\theta} + \frac{\delta}{2} \|\mathbf{A}\boldsymbol{\theta} - \boldsymbol{\eta} - \frac{1}{\delta} \boldsymbol{\zeta}\|_2^2.$$

Setting $\frac{\partial \mathcal{L}_n}{\partial \boldsymbol{\theta}} = 0$ leads to the update equation for $\boldsymbol{\theta}$. For a given estimate $(\boldsymbol{\eta}^{(s)}, \boldsymbol{\zeta}^{(s)})$ at the s th iteration, the $(s+1)$ th estimate of $\boldsymbol{\theta}$ is

$$\boldsymbol{\theta}^{(s+1)} = (\mathbf{H}^\top \mathbf{H} + \lambda_1 \mathbf{G} + \delta \mathbf{A}^\top \mathbf{A})^{-1} \left[\mathbf{H}^\top \mathbf{y} + \delta \mathbf{A}^\top (\boldsymbol{\eta}^{(s)} + \frac{1}{\delta} \boldsymbol{\zeta}^{(s)}) \right].$$

For $\boldsymbol{\eta}_{ij}$, the relevant component in L_n is

$$\frac{\delta}{2} \|\boldsymbol{\eta}_{ij} - \boldsymbol{\theta}_i + \boldsymbol{\theta}_j + \frac{1}{\delta} \boldsymbol{\zeta}_{ij}\|_2^2 + \rho_\tau (\|\boldsymbol{\eta}_{ij}\|_2, \omega_{ij} \lambda_2).$$

Hence, the close-form solution for the MCP penalty with $\tau > \frac{1}{\delta}$ is

$$\boldsymbol{\eta}_{ij}^{(s+1)} = \begin{cases} \mathbf{u}_{ij}^{(s+1)} & \text{if } \|\mathbf{u}_{ij}^{(s+1)}\|_2 \geq \tau \omega_{ij} \lambda_2, \\ \frac{\tau \delta}{\tau \delta - 1} \left(1 - \frac{\lambda_2}{\delta \|\mathbf{u}_{ij}^{(s+1)}\|_2} \right)_+ \mathbf{u}_{ij}^{(s+1)} & \text{if } \|\mathbf{u}_{ij}^{(s+1)}\|_2 < \tau \omega_{ij} \lambda_2, \end{cases}$$

where $\mathbf{u}_{ij}^{(s+1)} = \boldsymbol{\theta}_i^{(s+1)} - \boldsymbol{\theta}_j^{(s+1)} - \frac{1}{\delta} \boldsymbol{\zeta}_{ij}^{(s)}$, and $(x)_+ = x$ if $x > 0$ and $(x)_+ = 0$ otherwise. Finally, the estimate of $\boldsymbol{\eta}$ is updated as

$$\boldsymbol{\zeta}^{(s+1)} = \boldsymbol{\zeta}^{(s)} + \delta (\mathbf{A}\boldsymbol{\theta}^{(s+1)} - \boldsymbol{\eta}^{(s+1)}).$$

B. Proofs of Theorem 1 and 2

Proof of Theorem 1

By Theorem 3.1 of [6] and Conditions (C1)-(C3), we have

$$\mathbb{E}(\|\hat{\beta}_i^{\text{or}} - \beta_i^0\|_2^2) = O_p(\phi_{|\mathcal{G}_k|}).$$

As $\mathbb{E}^2(\|\hat{\beta}_i^{\text{or}} - \beta_i^0\|_2) \leq \mathbb{E}(\|\hat{\beta}_i^{\text{or}} - \beta_i^0\|_2^2)$, then

$$\text{Var}(\|\hat{\beta}_i^{\text{or}} - \beta_i^0\|_2) = \mathbb{E}(\|\hat{\beta}_i^{\text{or}} - \beta_i^0\|_2^2) - \mathbb{E}^2(\|\hat{\beta}_i^{\text{or}} - \beta_i^0\|_2) = O_p(\phi_{|\mathcal{G}_k|}).$$

Let $V_k = \text{Var}(\|\hat{\beta}_i^{\text{or}} - \beta_i^0\|_2)$ and $E_k = \mathbb{E}(\|\hat{\beta}_i^{\text{or}} - \beta_i^0\|_2)$. For any $\epsilon > 0$, there exists a constant C_ϵ^1 such that $\Pr(V_k > C_\epsilon^1 \phi_{|\mathcal{G}_k|}) \leq \epsilon$. By Chebyshev Inequality, $\Pr(\|\hat{\beta}_i^{\text{or}} - \beta_i^0\|_2 - E_k \geq \sigma) \leq \frac{V_k}{\sigma^2}$ for any $\sigma > 0$. Then

$$\begin{aligned} \Pr(\|\hat{\beta}_i^{\text{or}} - \beta_i^0\|_2 \geq \sigma) &\leq \Pr(\|\hat{\beta}_i^{\text{or}} - \beta_i^0\|_2 \geq \sigma, V_k \leq C_\epsilon^1 \phi_{|\mathcal{G}_k|}) + \Pr(V_k > C_\epsilon^1 \phi_{|\mathcal{G}_k|}) \\ &\leq \Pr(\|\hat{\beta}_i^{\text{or}} - \beta_i^0\|_2 - E_k + E_k \geq \sigma, V_k \leq C_\epsilon^1 \phi_{|\mathcal{G}_k|}) \\ &\quad + \Pr(V_k > C_\epsilon^1 \phi_{|\mathcal{G}_k|}) \\ &\leq \Pr(\|\hat{\beta}_i^{\text{or}} - \beta_i^0\|_2 - E_k \geq \frac{\sigma}{2}, V_k \leq C_\epsilon^1 \phi_{|\mathcal{G}_k|}) + \Pr(E_k \geq \frac{\sigma}{2}) \\ &\quad + \Pr(V_k > C_\epsilon^1 \phi_{|\mathcal{G}_k|}) \\ &\leq \frac{4C_\epsilon^1 \phi_{|\mathcal{G}_k|}}{\sigma^2} + \Pr(E_k \geq \frac{\sigma}{2}) + \epsilon. \end{aligned}$$

Under Condition (C4) and all assumptions in Theorem 1, we have $\phi_{|\mathcal{G}_k|} = O(|\mathcal{G}_{\min}|^{-a})$, where $a \in (\frac{1+\sigma_0}{4}, \frac{1-\sigma_0}{2}]$. Let $C_\epsilon^3 = 2(\epsilon^{-1}C_\epsilon^1)^{1/2}$ and $\sigma = C_\epsilon^3\phi_{|\mathcal{G}_k|}^{1/2}$. Then for sufficiently large $|\mathcal{G}_k|$, we have

$$\Pr(\|\hat{\beta}_i^{\text{or}} - \beta_i^0\|_2 \geq C_\epsilon^3\phi_{|\mathcal{G}_k|}^{1/2}) \leq 3\epsilon.$$

As a result, $\|\hat{\beta}_i^{\text{or}} - \beta_i^0\|_2 = O_p(\phi_{|\mathcal{G}_k|}^{1/2})$.

Proof of Theorem 2

Let $\rho(t) = \lambda_2^{-1}\rho_\tau(t, \lambda_2)$. Similar to [17], we define

$$L_n(\boldsymbol{\theta}) = \frac{1}{2}\|\mathbf{y} - \mathbf{H}\boldsymbol{\theta}\|_2^2, D_n(\boldsymbol{\theta}; \lambda_1) = \frac{1}{2}\lambda_1\boldsymbol{\theta}^\top \mathbf{G}\boldsymbol{\theta}, P_n(\boldsymbol{\theta}; \lambda_2) = \lambda_2 \sum_{i < j} \rho(\|\boldsymbol{\theta}_i - \boldsymbol{\theta}_j\|_2).$$

For simplicity, here we assume weight $w_{ij} = 1$ for all $1 \leq i < j \leq n$, and the following proof can be easily generalized to general w_{ij} 's. Then $Q_n(\boldsymbol{\theta}; \boldsymbol{\lambda}) = L_n(\boldsymbol{\theta}) + D_n(\boldsymbol{\theta}; \lambda_1) + P_n(\boldsymbol{\theta}; \lambda_2)$.

Define $T: \mathcal{M}_{\mathcal{G}} \rightarrow \mathbb{R}^{Kp}$ as a mapping, under which $T(\boldsymbol{\theta})$ is the Kp -vector consisting of K vectors with dimension p and its k th vector component equals the common value of $\boldsymbol{\theta}_i$ for $i \in \mathcal{G}_k$, and $T^*: \mathbb{R}^{Kp} \rightarrow \mathbb{R}^{Kp}$ as another mapping, under which $T^*(\boldsymbol{\theta}) = \{|\mathcal{G}_k|^{-1} \sum_{i \in \mathcal{G}_k} \boldsymbol{\theta}_i^\top, k \in \{1, \dots, K\}\}^\top$. Obviously, when $\boldsymbol{\theta} \in \mathcal{M}_{\mathcal{G}}$, $T(\boldsymbol{\theta}) = T^*(\boldsymbol{\theta})$.

Let $\boldsymbol{\theta}^0 = (\boldsymbol{\theta}_1^{0\top}, \dots, \boldsymbol{\theta}_n^{0\top})^\top$ be the true B-spline coefficient functions corresponding to the true subgroup set \mathcal{G} , and $\boldsymbol{\alpha}^0 = (\boldsymbol{\alpha}_1^{0\top}, \dots, \boldsymbol{\alpha}_K^{0\top})^\top$ be the distinct value of $\boldsymbol{\theta}^0$. Consider the neighborhood of $\boldsymbol{\theta}^0$:

$$\Theta = \{\boldsymbol{\theta} \in \mathbb{R}^{np} : \sup_i \|\boldsymbol{\theta}_i - \boldsymbol{\theta}_i^0\|_2 \leq \Lambda_n \triangleq \phi_{|\mathcal{G}_k|}^{1/2} m^{1/2} = o(1).\}$$

By Theorem 26 of [15], there exist constants $c_{m,q} > 0$, which are only dependent on m and q , such that for $1 \leq i \leq n$,

$$c_{m,q}\|\hat{\boldsymbol{\theta}}_i^{\text{or}} - \boldsymbol{\theta}_i^0\|_2 \leq \|\mathbf{B}(\hat{\boldsymbol{\theta}}_i^{\text{or}} - \boldsymbol{\theta}_i^0)\|_2 = \|\hat{\beta}_i^{\text{or}} - \mathbf{B}\boldsymbol{\theta}_i^0\|_2 \leq \|\hat{\beta}_i^{\text{or}} - \beta_i^0\|_2 + \|\beta_i^0 - \mathbf{B}\boldsymbol{\theta}_i^0\|_2, \quad (12)$$

where $c_{m,q} \sim q^{-1}m^{-1/2}$. Note that the B-spline order q is a constant. By (B.7) (Lemma 1), $\|\beta_i^0 - \mathbf{B}\boldsymbol{\theta}_i^0\|_2 = o(\|\hat{\beta}_i^{\text{or}} - \beta_i^0\|_2)$. Therefore, by Theorem 1, we have $\Pr(\hat{\boldsymbol{\theta}}^{\text{or}} \in \Theta) \rightarrow 1$. For any $\boldsymbol{\theta} \in \mathcal{R}^{np}$, let $T^*(\boldsymbol{\theta}) = \boldsymbol{\alpha} = (\boldsymbol{\alpha}_1^\top, \dots, \boldsymbol{\alpha}_K^\top)^\top$ and $\boldsymbol{\theta}^* = T^{-1}(T^*(\boldsymbol{\theta})) = T^{-1}(\boldsymbol{\alpha})$.

We will show that $\hat{\boldsymbol{\theta}}^{\text{or}}$ is a strictly local minimizer of the objective function $Q_n(\boldsymbol{\theta}; \boldsymbol{\lambda})$ with probability approaching 1 through the following two steps:

- (i) $Q_n(\boldsymbol{\theta}^*; \boldsymbol{\lambda}) > Q_n(\hat{\boldsymbol{\theta}}^{\text{or}}; \boldsymbol{\lambda})$ for any $\boldsymbol{\theta} \in \Theta$ and $\boldsymbol{\theta}^* \neq \boldsymbol{\theta}^{\text{or}}$.
- (ii) For any $\boldsymbol{\theta} \in \Theta$, $Q_n(\boldsymbol{\theta}; \boldsymbol{\lambda}) \geq Q_n(\boldsymbol{\theta}^*; \boldsymbol{\lambda})$ with probability approaching 1.

We first prove the results in (i). Since $\hat{\boldsymbol{\theta}}^{\text{or}}$ is the global minimizer of $L_n(\boldsymbol{\theta}) + D_n(\boldsymbol{\theta}; \lambda_1)$ for $\boldsymbol{\theta} \in \mathcal{M}_{\mathcal{G}}$, then $L_n(\boldsymbol{\theta}^*) + D_n(\boldsymbol{\theta}^*; \lambda_1) > L_n(\hat{\boldsymbol{\theta}}^{\text{or}}) + D_n(\hat{\boldsymbol{\theta}}^{\text{or}}; \lambda_1)$. Hence we only need to consider $P_n(\boldsymbol{\theta}^*; \lambda_2)$. Again by Theorem 26 of [15], there exist constants $c_m \sim m^{-1/2}$, such that for $1 \leq k \leq K$,

$$\|\mathbf{B}\boldsymbol{\alpha}_k^0 - \mathbf{B}\boldsymbol{\alpha}_{k'}^0\|_2 \leq c_m\|\boldsymbol{\alpha}_k^0 - \boldsymbol{\alpha}_{k'}^0\|_2.$$

Similarly, we have

$$\|\xi_k^0 - \xi_{k'}^0\|_2 \leq \|\mathbf{B}\boldsymbol{\alpha}_k^0 - \mathbf{B}\boldsymbol{\alpha}_{k'}^0\|_2 + \|\mathbf{B}\boldsymbol{\alpha}_k^0 - \xi_k^0\|_2 + \|\mathbf{B}\boldsymbol{\alpha}_{k'}^0 - \xi_{k'}^0\|_2,$$

where $\|\mathbf{B}\boldsymbol{\alpha}_k^0 - \xi_k^0\|_2 = o(\|\hat{\xi}_k^{\text{or}} - \xi_k^0\|_2)$ and $\|\mathbf{B}\boldsymbol{\alpha}_{k'}^0 - \xi_{k'}^0\|_2 = o(\|\hat{\xi}_{k'}^{\text{or}} - \xi_{k'}^0\|_2)$. Thus $\|\boldsymbol{\alpha}_k^0 - \boldsymbol{\alpha}_{k'}^0\|_2 \geq c\|\xi_k^0 - \xi_{k'}^0\|_2 \geq cb$ for

sufficiently large n . Then,

$$\begin{aligned}
\|\alpha_k - \alpha_{k'}\|_2 &\geq \|\alpha_k^0 - \alpha_{k'}^0\|_2 - \|\alpha_k - \alpha_k^0\|_2 - \|\alpha_{k'}^0 - \alpha_{k'}\|_2 \\
&\geq \|\alpha_k^0 - \alpha_{k'}^0\|_2 - 2\sup_j \|\alpha_j - \alpha_j^0\|_2 \\
&\geq cb - 2\sup_j \|\mathcal{G}_j\|^{-1} \sum_{i \in \mathcal{G}_j} (\theta_i - \theta_i^0) \|_2 \\
&\geq cb - 2\sup_j \|\mathcal{G}_j\|^{-1} \sum_{i \in \mathcal{G}_j} \|\theta_i - \theta_i^0\|_2 \\
&\geq cb - 2\sup_i \|\theta_i - \theta_i^0\|_2 \\
&\geq cb - 2\Lambda_n \\
&> a\lambda_2,
\end{aligned} \tag{13}$$

where the last inequality follows from the assumption that $cb > a\lambda_2 \gg \Lambda_n$. Consequently, $\rho(\|\alpha_k - \alpha_{k'}\|_2)$ is a constant by (C5). Since

$$P_n(\theta^*; \lambda_2) = \lambda_2 \sum_{i < j} \rho(\|\theta_i^* - \theta_j^*\|_2) = \lambda_2 \sum_{k \neq k'} \frac{|\mathcal{G}_k| |\mathcal{G}_{k'}|}{2} \rho(\|\alpha_k - \alpha_{k'}\|_2),$$

then $P_n(\theta^*; \lambda_2) = C_n$ where C_n is a constant. Therefore, $L_n(\theta^*) + D_n(\theta^*; \lambda_1) + C_n > L_n(\hat{\theta}^{\text{or}}) + D_n(\hat{\theta}^{\text{or}}; \lambda_1) + C_n$, that is, $Q_n(\theta^*; \lambda) > Q_n(\hat{\theta}^{\text{or}}; \lambda)$, for all $\theta^* \neq \hat{\theta}^{\text{or}}$. The result in (i) is proved.

Now we prove the results in (ii). For $\theta \in \Theta$, by Taylor's expansion, we have

$$Q_n(\theta; \lambda) - Q_n(\theta^*; \lambda) = \Gamma_1 + \Gamma_2 + \Gamma_3,$$

where $\Gamma_1 = -(\mathbf{y} - \mathbf{H}\theta^m)^\top \mathbf{H}(\theta - \theta^*)$, $\Gamma_2 = \lambda_1 \theta^{m\top} \mathbf{G}(\theta - \theta^*)$, $\Gamma_3 = \frac{\partial P_n(\theta; \lambda_2)}{\partial \theta} \Big|_{\theta=\theta^m} (\theta - \theta^*)$, and $\theta^m = c\theta + (1-c)\theta^*$ for some constant $c \in (0, 1)$.

Let $-\mathbf{H}^\top(\mathbf{y} - \mathbf{H}\theta^m) = \mathbf{w} = (\mathbf{w}_1^\top, \mathbf{w}_2^\top, \dots, \mathbf{w}_n^\top)^\top$. Then

$$\begin{aligned}
\Gamma_1 = \mathbf{w}^\top (\theta - \theta^*) &= \sum_{i=1}^n \mathbf{w}_i^\top (\theta_i - \theta_i^*) = \sum_{k=1}^K \sum_{\{i,j \in \mathcal{G}_k, i < j\}} \frac{(\mathbf{w}_i - \mathbf{w}_j)^\top (\theta_i - \theta_j)}{|\mathcal{G}_k|} \\
&\geq - \sum_{k=1}^K \sum_{\{i,j \in \mathcal{G}_k, i < j\}} \frac{2\sup_i \|\mathbf{w}_i\|_2 \cdot \|\theta_i - \theta_j\|_2}{|\mathcal{G}_{\min}|},
\end{aligned} \tag{14}$$

where the third equality is obtained from $\theta^* = T^{-1}(T^*(\theta))$ and $\sum_{i=1}^n \omega_i^\top \theta_i^* = \sum_{k=1}^K \frac{1}{|\mathcal{G}_k|} \sum_{i,j \in \mathcal{G}_k} \omega_i^\top \theta_j$.

Let $\lambda_1 \mathbf{G}\theta^m = \mathbf{v} = (\mathbf{v}_1^\top, \dots, \mathbf{v}_n^\top)^\top$. Then

$$\Gamma_2 = \mathbf{v}^\top (\theta - \theta^*) \geq - \sum_{k=1}^K \sum_{\{i,j \in \mathcal{G}_k, i < j\}} \frac{2\sup_i \|\mathbf{v}_i\|_2 \cdot \|\theta_i - \theta_j\|_2}{|\mathcal{G}_{\min}|}. \tag{15}$$

$$\begin{aligned}
\Gamma_3 &= \frac{\partial P_n(\theta; \lambda_2)}{\partial \theta} \Big|_{\theta=\theta^m} (\theta - \theta^*) \\
&= \lambda_2 \sum_{i < j} \rho'(\|\theta_i^m - \theta_j^m\|_2) \frac{(\theta_i^m - \theta_j^m)^\top}{\|\theta_i^m - \theta_j^m\|_2} [(\theta_i - \theta_i^*) - (\theta_j - \theta_j^*)].
\end{aligned}$$

Recall that $\sup_i \|\theta_i - \theta_i^0\|_2 \leq \Lambda_n$ for $\theta \in \Theta$. By the same reasoning as (13), we have $\sup_k \|\alpha_k - \alpha_k^0\|_2 \leq \Lambda_n$. Then $\sup_i \|\theta_i^* - \theta_i^0\|_2 \leq \Lambda_n$. Since θ^m is between θ and θ^* , we have

$$\sup_i \|\theta_i^m - \theta_i^0\|_2 \leq \Lambda_n. \tag{16}$$

Hence for $i \in \mathcal{G}_k, j \in \mathcal{G}_{k'}, k \neq k'$,

$$\begin{aligned} \|\boldsymbol{\theta}_i^m - \boldsymbol{\theta}_j^m\|_2 &\geq \|\boldsymbol{\theta}_i^0 - \boldsymbol{\theta}_j^0\|_2 - 2\sup_l \|\boldsymbol{\theta}_l^m - \boldsymbol{\theta}_l^0\|_2 \\ &= \|\boldsymbol{\alpha}_k^0 - \boldsymbol{\alpha}_{k'}^0\|_2 - 2\sup_l \|\boldsymbol{\theta}_l^m - \boldsymbol{\theta}_l^0\|_2 \\ &\geq b - 2\Lambda_n > a\lambda_2, \end{aligned}$$

and thus $\rho'(\|\boldsymbol{\theta}_i^m - \boldsymbol{\theta}_j^m\|_2) = 0$. Consequently,

$$\Gamma_3 = \lambda_2 \sum_{k=1}^K \sum_{i,j \in \mathcal{G}_k, i < j} \rho'(\|\boldsymbol{\theta}_i^m - \boldsymbol{\theta}_j^m\|_2) \frac{(\boldsymbol{\theta}_i^m - \boldsymbol{\theta}_j^m)^\top}{\|\boldsymbol{\theta}_i^m - \boldsymbol{\theta}_j^m\|_2} [(\boldsymbol{\theta}_i - \boldsymbol{\theta}_i^*) - (\boldsymbol{\theta}_j - \boldsymbol{\theta}_j^*)].$$

When $i, j \in \mathcal{G}_k, \boldsymbol{\theta}_i^* = \boldsymbol{\theta}_j^*$ and $\boldsymbol{\theta}_i^m - \boldsymbol{\theta}_j^m = c(\boldsymbol{\theta}_i - \boldsymbol{\theta}_j)$. Thus

$$\Gamma_3 = \lambda_2 \sum_{k=1}^K \sum_{i,j \in \mathcal{G}_k, i < j} \rho'(\|\boldsymbol{\theta}_i^m - \boldsymbol{\theta}_j^m\|_2) \|\boldsymbol{\theta}_i - \boldsymbol{\theta}_j\|_2.$$

Further,

$$\begin{aligned} \sup_k \sup_{i,j \in \mathcal{G}_k} \|\boldsymbol{\theta}_i^m - \boldsymbol{\theta}_j^m\|_2 &= \sup_k \sup_{i,j \in \mathcal{G}_k} \|\boldsymbol{\theta}_i^m - \boldsymbol{\theta}_i^* + \boldsymbol{\theta}_i^* - \boldsymbol{\theta}_j^* + \boldsymbol{\theta}_j^* - \boldsymbol{\theta}_j^m\|_2 \\ &\leq 2\sup_i \|\boldsymbol{\theta}_i^m - \boldsymbol{\theta}_i^*\|_2 \leq 4\Lambda_n. \end{aligned}$$

By the concavity of $\rho(\cdot)$,

$$\Gamma_3 \geq \sum_{k=1}^K \sum_{\{i,j \in \mathcal{G}_k, i < j\}} \lambda_2 \rho'(4\Lambda_n) \|\boldsymbol{\theta}_i - \boldsymbol{\theta}_j\|_2. \quad (17)$$

Therefore, with (14), (15), and (17), we have

$$\begin{aligned} Q_n(\boldsymbol{\theta}; \boldsymbol{\lambda}) - Q_n(\boldsymbol{\theta}^*, \boldsymbol{\lambda}) &= \Gamma_1 + \Gamma_2 + \Gamma_3 \\ &\geq \sum_{k=1}^K \sum_{\{i,j \in \mathcal{G}_k, i < j\}} \|\boldsymbol{\theta}_i - \boldsymbol{\theta}_j\|_2 \left[\lambda_2 \rho'(4\Lambda_n) - 2 \frac{\sup_i \|\mathbf{w}_i\|_2 + \sup_i \|\mathbf{v}_i\|_2}{|\mathcal{G}_{\min}|} \right] \end{aligned}$$

By Lemma 1, we have $\lambda_2 \gg \frac{\sup_i \|\mathbf{w}_i\|_2 + \sup_i \|\mathbf{v}_i\|_2}{|\mathcal{G}_{\min}|}$ with probability approaching 1. Since $\rho'(4\Lambda_n) \rightarrow 1$, we have

$$Q_n(\boldsymbol{\theta}; \boldsymbol{\lambda}) - Q_n(\boldsymbol{\theta}^*, \boldsymbol{\lambda}) \geq 0$$

with probability approaching 1, so that the result in (ii) is proved. Therefore, there exists a local minimizer $\hat{\boldsymbol{\theta}}$ of the objective function $Q_n(\boldsymbol{\theta}; \boldsymbol{\lambda})$, such that $\Pr(\hat{\boldsymbol{\theta}} = \hat{\boldsymbol{\theta}}^{\text{or}}) \rightarrow 1$. By (12), we can conclude that there exists a local minimizer $\hat{\boldsymbol{\beta}}$ of the objective function $Q_n(\boldsymbol{\theta}; \boldsymbol{\lambda})$ such that $\Pr(\hat{\boldsymbol{\beta}} = \hat{\boldsymbol{\beta}}^{\text{or}}) \rightarrow 1$.

Lemma 1. Under Conditions (C1)-(C3), \mathbf{w} and \mathbf{v} are defined in the proof of Theorem 2, we have $\lambda_2 \gg \frac{\sup_i \|\mathbf{w}_i\|_2 + \sup_i \|\mathbf{v}_i\|_2}{|\mathcal{G}_{\min}|}$ with probability approaching 1.

Proof. Let $s_i = \mathbf{B}\boldsymbol{\theta}_i^0$. Define $e_i = \beta_i^0 - s_i$ and $e_{i2} = (\beta_i^0)'' - s_i''$. By Theorem 48 of [15], we have

$$\begin{aligned} \|e_i\|_2 &\leq C_q \left(\frac{T}{m}\right)^{q-2} \|\beta_i^{0(q-2)}\|_2, \\ \|e_{i2}\|_2 &\leq C_q \left(\frac{T}{m}\right)^{q-4} \|\beta_i^{0(q-2)}\|_2, \end{aligned} \quad (18)$$

where C_q is a constant depending only on q , and $\beta_i^{(q-2)}$ is the $(q-2)$ -th derivative of β_i . Let $E_i = \int_{\mathcal{X}} X_i(t)e_i(t)dt$. Then $y_i = \mathbf{H}_i\theta_i^0 + E_i + \epsilon_i$, and hence

$$\begin{aligned} \mathbf{w}_i &= -\mathbf{H}_i^\top (y_i - \mathbf{H}_i\theta_i^m) \\ &= \mathbf{H}_i^\top \mathbf{H}_i(\theta_i^m - \theta_i^0) - \mathbf{H}_i^\top E_i - \mathbf{H}_i^\top \epsilon_i \end{aligned}$$

According to Lemma 8 from [10],

$$\sum_{l=1}^p \|B_l\|_2^2 = \int_{\mathcal{X}} \sum_{l=1}^p (B_l(t))^2 dt \leq \int_{\mathcal{X}} \sum_{l=1}^p B_l(t) dt \leq T. \quad (19)$$

Since $\sup_i \|\theta_i^m - \theta_i^0\|_2 \leq \Lambda_n$, (19) and $H_i = (\int_{\mathcal{X}} X_i(t)B_1(t)dt, \dots, \int_{\mathcal{X}} X_i(t)B_p(t)dt)$, then

$$\begin{aligned} \|\mathbf{H}_i^\top \mathbf{H}_i(\theta_i^m - \theta_i^0)\|_2 &\leq \|\mathbf{H}_i^\top \mathbf{H}_i\|_F \|\theta_i^m - \theta_i^0\|_2 \\ &\leq \Lambda_n \sum_{l=1}^p \left(\int_{\mathcal{X}} X_i(t)B_l(t)dt \right)^2 \\ &\leq \Lambda_n \|X_i\|_2^2 \sum_{l=1}^p \|B_l\|_2^2 \\ &\leq T \Lambda_n \|X_i\|_2^2. \end{aligned} \quad (20)$$

Since

$$\mathbf{H}_i^\top E_i = \left(\int_{\mathcal{X}} X_i(t)B_1(t)dt \int_{\mathcal{X}} X_i(t)e_i(t)dt, \dots, \int_{\mathcal{X}} X_i(t)B_p(t)dt \int_{\mathcal{X}} X_i(t)e_i(t)dt \right)^\top,$$

thus

$$\begin{aligned} &\|\mathbf{H}_i^\top E_i\|_2 \\ &= \sqrt{\left(\int_{\mathcal{X}} X_i(t)e_i(t)dt \right)^2 \left[\left(\int_{\mathcal{X}} X_i(t)B_1(t)dt \right)^2 + \dots + \left(\int_{\mathcal{X}} X_i(t)B_p(t)dt \right)^2 \right]} \\ &\leq \|X_i\|_2 \sqrt{\sum_{l=1}^p \|B_l\|_2^2} \int_{\mathcal{X}} X_i(t)e_i(t)dt \\ &\leq \sqrt{T} \|X_i\|_2^2 \|e_i\|_2, \end{aligned} \quad (21)$$

Since

$$\mathbf{H}_i^\top \epsilon_i = \left(\epsilon_i \int_{\mathcal{X}} X_i(t)B_1(t)dt, \dots, \epsilon_i \int_{\mathcal{X}} X_i(t)B_p(t)dt \right)^\top,$$

then

$$\begin{aligned} \|\mathbf{H}_i^\top \epsilon_i\|_2 &= \sqrt{\epsilon_i^2 \left(\int_{\mathcal{X}} X_i(t)B_1(t)dt \right)^2 + \dots + \epsilon_i^2 \left(\int_{\mathcal{X}} X_i(t)B_p(t)dt \right)^2} \\ &\leq |\epsilon_i| \|X_i\|_2 \sqrt{\sum_{l=1}^p \|B_l\|_2^2} \\ &\leq \sqrt{T} |\epsilon_i| \|X_i\|_2. \end{aligned} \quad (22)$$

Therefore, with (20), (21), and (22), we have,

$$\|\mathbf{w}_i\|_2 \leq \sqrt{T} \|X_i\|_2 (\sqrt{T} \Lambda_n \|X_i\|_2 + \|X_i\|_2 \|e_i\|_2 + |\epsilon_i|).$$

Since $\Pr(|\epsilon_i| > C\sqrt{p}) \leq \frac{\sigma^2}{C^2 p}$ for any positive constant C , then, by Condition (C1) and assumption in Theorem 1, $|\epsilon_i| = o_p(\sqrt{p})$. Recall $\Lambda_n = o(1)$. Therefore, by Condition (C2)-(C3) and (18),

$$\sup_i \|\mathbf{w}_i\|_2 = o_p(1). \quad (23)$$

Recall $\mathbf{v} = (\mathbf{v}_1^\top, \dots, \mathbf{v}_n^\top)^\top = \lambda_1 \mathbf{G} \boldsymbol{\theta}^m$ and $\mathbf{G} = \mathbf{I}_n \otimes \mathbf{G}_0$, then

$$\mathbf{v}_i = \lambda_1 \mathbf{G}_0 \boldsymbol{\theta}_i^m = \lambda_1 \mathbf{G}_0 (\boldsymbol{\theta}_i^m - \boldsymbol{\theta}_i^0) + \lambda_1 \mathbf{G}_0 \boldsymbol{\theta}_i^0,$$

and hence

$$\|\mathbf{v}_i\|_2 \leq \lambda_1 \|\mathbf{G}_0 (\boldsymbol{\theta}_i^m - \boldsymbol{\theta}_i^0)\|_2 + \lambda_1 \|\mathbf{G}_0 \boldsymbol{\theta}_i^0\|_2.$$

By the definition of \mathbf{G}_0 , we have

$$\begin{aligned} \|\mathbf{G}_0 (\boldsymbol{\theta}_i^m - \boldsymbol{\theta}_i^0)\|_2 &\leq \|\mathbf{G}_0\|_F \|\boldsymbol{\theta}_i^m - \boldsymbol{\theta}_i^0\|_2 \\ &\leq \Lambda_n \sqrt{\sum_{l_1=1}^p \sum_{l_2=1}^p \left(\int_{\mathcal{X}} B_{l_1}''(t) B_{l_2}''(t) dt \right)^2} \\ &\leq p \Lambda_n \sup_{1 \leq l \leq p} \{\|B_l''\|_2^2\}, \end{aligned} \quad (24)$$

where the second inequality follows from (16). Since

$$\mathbf{G}_0 \boldsymbol{\theta}_i^0 = \left(\int_{\mathcal{X}} \sum_{l=1}^p B_l''(t) B_l''(t) \theta_{il}^0 dt, \dots, \int_{\mathcal{X}} \sum_{l=1}^p B_p''(t) B_l''(t) \theta_{il}^0 dt \right)^\top,$$

then

$$\begin{aligned} \|\mathbf{G}_0 \boldsymbol{\theta}_i^0\|_2 &= \sqrt{\left(\int_{\mathcal{X}} B_1''(t) s_{p1}''(t) dt \right)^2 + \dots + \left(\int_{\mathcal{X}} B_p''(t) s_{p1}''(t) dt \right)^2} \\ &\leq \sqrt{\int_{\mathcal{X}} B_1''(t)^2 dt \int_{\mathcal{X}} s_1''(t)^2 dt + \dots + \int_{\mathcal{X}} B_p''(t)^2 dt \int_{\mathcal{X}} s_1''(t)^2 dt} \\ &\leq \sqrt{p \sup_l \{ \int_{\mathcal{X}} B_l''(t)^2 dt \} \int_{\mathcal{X}} s_i''(t)^2 dt} \\ &= \sqrt{p \sup_l \{ \|B_l''\|_2^2 \} \|\beta_i^{0''}(t) - e_{i2}(t)\|_2^2} \end{aligned} \quad (25)$$

Therefore, with (24) and (25), we have

$$\|\mathbf{v}_i\|_2 \leq \lambda_1 \sup_l \{\|B_l''(t)\|_2\} (\sqrt{p} \|\beta_i^{0''}(t) - e_{i2}(t)\|_2 + p \Lambda_n \sup_l \{\|B_l''(t)\|_2\}).$$

According to the derivative of B-spline function given in [2], we have $\sup_l \{\|B_l''\|_2^2\} \sim p^3$. Moreover, by (18), $\|\beta_i^{0''} - e_{i2}\|_2 \sim \|\beta_i^{0''}\|_2$. Recall $\Lambda_n = o(1)$. Consequently, under Conditions (C2)-(C3),

$$\sup_i \|\mathbf{v}_i\|_2 = o(\lambda_1 p^4). \quad (26)$$

With (23) and (26), we have

$$\frac{\sup_i \|\mathbf{w}_i\|_2 + \sup_i \|\mathbf{v}_i\|_2}{|\mathcal{G}_{\min}|} = o\left(\frac{\lambda_1 p^4}{|\mathcal{G}_{\min}|}\right)$$

with probability approaching 1. Recall (C4) and $\lambda_2 \gg \frac{n^{-(1-\sigma_0)/2} p^4}{|\mathcal{G}_{\min}|}$. Therefore, we have $\lambda_2 \gg \frac{\sup_i \|\mathbf{w}_i\|_2 + \sup_i \|\mathbf{v}_i\|_2}{|\mathcal{G}_{\min}|}$ with probability approaching 1. \square

C. Tables and Figures

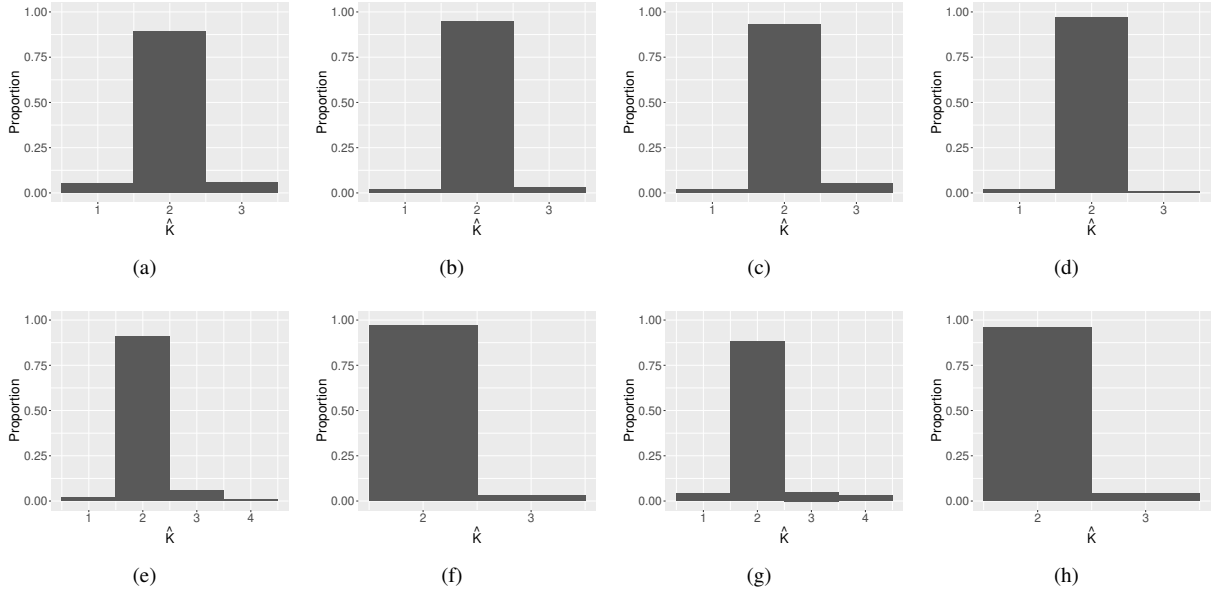


Fig. C1: Simulation results in Example 1: histograms of the estimated number of subgroups \hat{K} under Scenario 2. (a) and (e) balanced structure with $n = 40$, (b) and (f) balanced structure with $n = 200$, (c) and (g) unbalanced structure with $n = 40$, (d) and (h) unbalanced structure with $n = 200$. (a)-(d) $a_{il} \sim N(2, 1)$, and (b)-(h) $a_{il} \sim U(0, 4)$.

Figure C1 shows the distribution of the number of identified subgroups \hat{K} for Scenario 2 in Example 1. The proposed approach can satisfactorily identify the number of true subgroups for all settings. As n increases, the percentage of correctly determining the number of subgroups becomes larger.

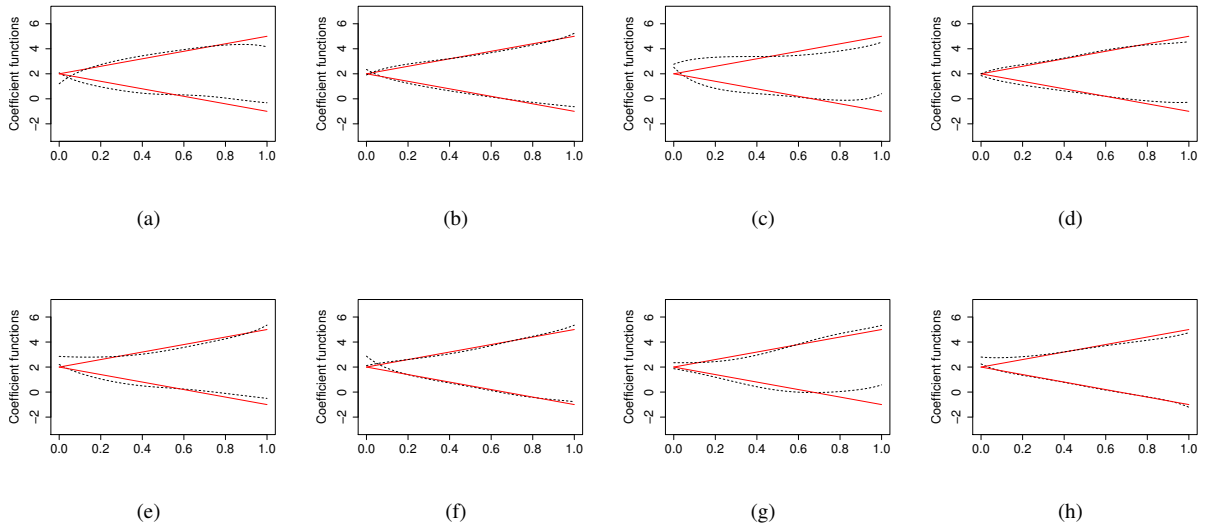


Fig. C2: Simulation results in Example 1: estimation of the coefficient functions under Scenario 2. (a) and (e) balanced structure with $n = 40$, (b) and (f) balanced structure with $n = 200$, (c) and (g) unbalanced structure with $n = 40$, (d) and (h) unbalanced structure with $n = 200$. (a)-(d) $a_{il} \sim N(2, 1)$, and (b)-(h) $a_{il} \sim U(0, 4)$. Red solid lines represent the true coefficient functions, and black dashed lines represent the estimated coefficient functions.

Figure C2 presents estimations of the coefficient functions for Scenario 2 in Example 1. It can be observed that the underlying true coefficient function curves can be recovered well.

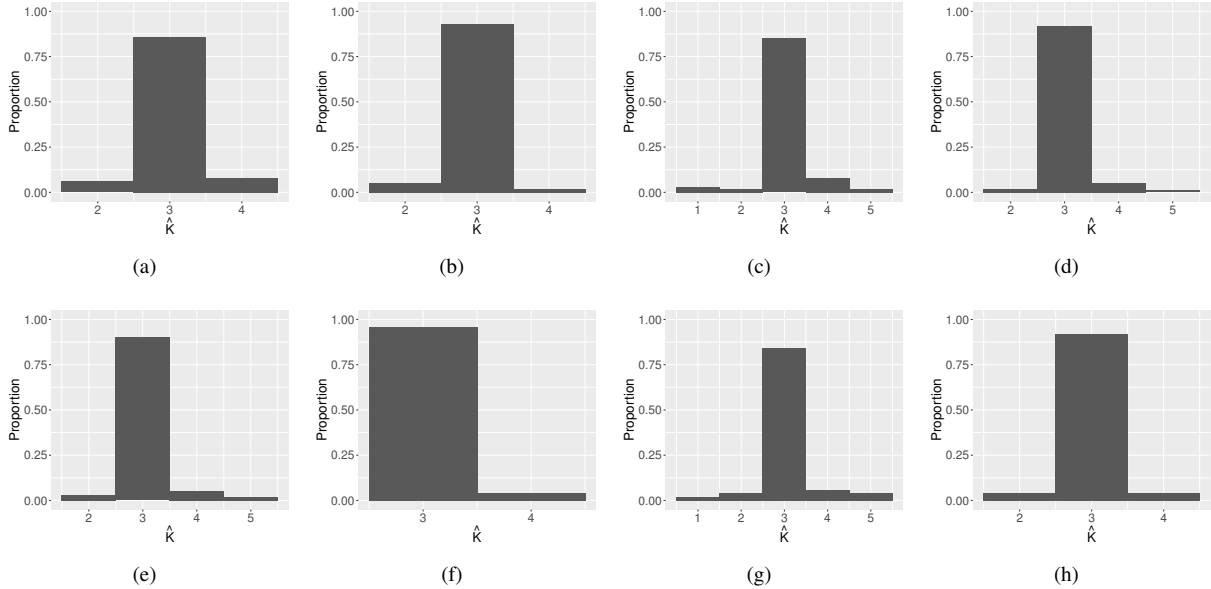


Fig. C3: Simulation results in Example 2: histograms of the estimated number of subgroups \hat{K} by the proposed approach. (a) and (e) balanced structure with $n = 60$, (b) and (f) balanced structure with $n = 300$, (c) and (g) unbalanced structure with $n = 60$, (d) and (h) unbalanced structure with $n = 300$. (a)-(d) $a_{il} \sim N(2, 1)$, and (b)-(h) $a_{il} \sim U(0, 4)$.

Figure C3 illustrates the distribution of the estimated number of subgroups by the proposed approach. We obtain similar patterns as those in Example 1. Again, the proposed approach can accurately identify the true number of subgroups.

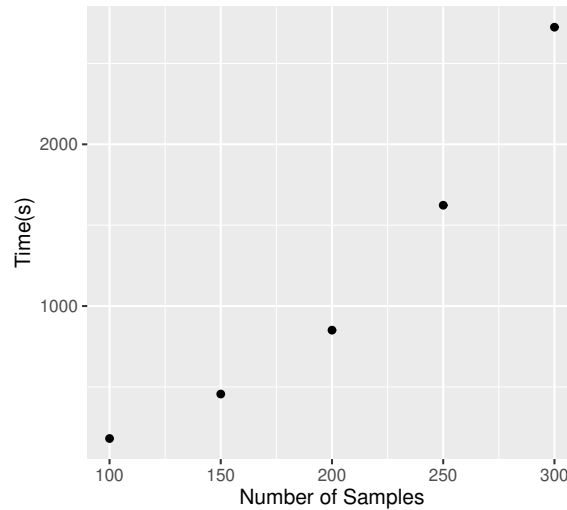


Fig. C4: The consumed time (in seconds) of each experiment with different number of samples.

Figure C4 illustrates the consumed time (in seconds) running our algorithm with different sample sizes. It can be seen that the consumed time rapidly increases at a nearly $O(n^2)$ speed as the sample size increases. Therefore, in

Table C1: Simulation results in Example 1: ARI and MSE based on 100 replications under Scenario 2.

Structure	a_{ij}	Method	$n = 40$		$n = 200$	
			ARI	MSE	ARI	MSE
B	Norm	Proposed	0.959(0.003)	1.063(0.091)	0.991(0.001)	0.216(0.014)
		Oracle		0.911(0.082)		0.205(0.012)
		FIMR	0.633(0.032)	39.492(5.284)	0.844(0.011)	7.877(2.298)
		Resp	0.942(0.005)	1.617(0.122)	0.964(0.002)	0.462(0.024)
		Resi	0.893(0.008)	2.932(0.376)	0.967(0.004)	0.731(0.059)
	Unif	Proposed	0.969(0.004)	0.977(0.084)	0.996(0.001)	0.254(0.015)
		Oracle		0.835(0.105)		0.232(0.012)
		FIMR	0.664(0.022)	47.027(7.523)	0.893(0.023)	4.295(2.010)
		Resp	0.935(0.005)	1.542(0.096)	0.965(0.002)	0.360(0.017)
		Resi	0.909(0.007)	1.923(0.184)	0.974(0.003)	0.347(0.029)
UB	Norm	Proposed	0.964(0.002)	1.124(0.096)	0.995(0.001)	0.341(0.014)
		Oracle		0.853(0.071)		0.255(0.013)
		FIMR	0.749(0.016)	25.827(5.638)	0.972(0.011)	3.522(1.296)
		Resp	0.938(0.007)	1.817(0.124)	0.973(0.003)	0.563(0.026)
		Resi	0.923(0.004)	1.931(0.168)	0.967(0.002)	0.523(0.023)
	Unif	Proposed	0.968(0.007)	1.230(0.102)	0.989(0.002)	0.381(0.015)
		Oracle		1.014(0.096)		0.386(0.015)
		FIMR	0.788(0.013)	27.352(4.985)	0.974(0.009)	3.369(1.074)
		Resp	0.946(0.009)	1.815(0.126)	0.952(0.004)	0.667(0.017)
		Resi	0.919(0.010)	2.043(0.198)	0.980(0.004)	0.422(0.024)

empirical studies, we randomly sampled 400 monitoring stations to reduce the computation cost.

Subgrouping and estimation results for Scenario 2 in Example 1 are summarized in Table C1. We obtain similar results as in Scenario 1 in the main manuscript. Since the Oracle approach assumes the true subgroup structure, the proposed approach behaves inferior to the Oracle as expected. But it has significant advantages over the FIMR, Resp and Resi approaches. The values of ARI and MSE increase as n grows for the proposed approach. This supports the estimation consistency established in Theorem 1 and 2.

Table C2 summarizes the results of subgrouping and estimation in Example 2. Similar to Example 1, aside from the Oracle approach, the ARI of the proposed approach is always the highest; therefore, it outperforms alternatives in the accuracy of identifying subgroup memberships. In terms of estimation accuracy, the proposed approach is again observed to have favorable performance. Compared to Example 1 where there are only two subgroups, here, the advantages of the proposed approach in terms of subgrouping and estimation are more significant. Consider for example $n = 60$, balanced structure, and a_{ij} 's are generated from norm distribution $N(2, 1)$. The proposed approach has (ARI, MSE)=(0.948, 1.969), which is superior to the alternatives: (0.533, 395.569) for the FIMR approach, (0.834, 4.230) for the Resp approach, and (0.781, 7.304) for the Resi approach. FIMR has the worst performance.

Table C3 presents the Normalized Mutual Information (NMI) which measures the similarity between the subgrouping results, with range $[0, 1]$ and a larger value indicating a higher degree of similarity. We find that the proposed approach has low similarity with the alternatives because the NMIs are low.

References

- [1] C. Blanchard, G. Hidy, Effects of so₂ and no_x emission reductions on pm_{2.5} mass concentrations in the southeastern united states, Journal of the Air and Waste Management Association 55 (2005) 265–272.

Table C2: Simulation results in Example 2: ARI and MSE. Each cell shows the mean(s.d.).

Structure	a_{ij}	Method	$n = 60$		$n = 300$	
			ARI	MSE	ARI	MSE
B	Norm	Proposed	0.948(0.006)	1.969(0.508)	0.969(0.001)	0.877(0.021)
		Oracle		1.096(0.104)		0.550(0.018)
		FIMR	0.533(0.028)	395.569(38.380)	0.789(0.013)	32.836(7.746)
		Resp	0.834(0.009)	4.230(0.344)	0.855(0.002)	2.317(0.052)
		Resi	0.781(0.018)	7.304(1.103)	0.937(0.003)	1.606(0.122)
	Unif	Proposed	0.958(0.007)	1.332(0.115)	0.996(0.002)	0.724(0.027)
		Oracle		0.977(0.051)		0.341(0.019)
		FIMR	0.588(0.025)	402.457(42.825)	0.763(0.021)	24.294(5.283)
		Resp	0.772(0.016)	6.269(0.481)	0.795(0.009)	2.997(0.153)
		Resi	0.752(0.015)	10.045(1.225)	0.903(0.003)	1.846(0.127)
UB	Norm	Proposed	0.944(0.005)	1.627(0.178)	0.987(0.002)	0.906(0.022)
		Oracle		0.921(0.098)		0.415(0.020)
		FIMR	0.611(0.030)	284.565(28.210)	0.876(0.012)	9.397(1.942)
		Resp	0.608(0.025)	6.386(0.553)	0.694(0.016)	4.142(0.279)
		Resi	0.751(0.016)	7.336(0.751)	0.825(0.005)	2.618(0.197)
	Unif	Proposed	0.954(0.008)	1.511(0.285)	0.970(0.002)	0.739(0.024)
		Oracle		1.042(0.138)		0.412(0.015)
		FIMR	0.632(0.027)	269.922(25.686)	0.843(0.021)	13.415(2.840)
		Resp	0.619(0.012)	7.991(0.368)	0.677(0.008)	5.124(0.481)
		Resi	0.787(0.017)	7.193(0.815)	0.863(0.005)	2.354(0.125)

Table C3: Data analysis: comparison of grouping results. In each cell, the value of NMI.

	Proposed	FIMR	Resp	Resi
Proposed	1	0.092	0.203	0.150
FIMR		1	0.126	0.183
Resp			1	0.336
Resi				1

- [2] C. Boor, A practical guide to splines, Applied Mathematical Sciences, Vol. 27, Springer, 1978.
- [3] D. Bosq, Linear processes in function spaces : theory and applications, Lecture Notes in Statistics 149 (2000) 181–202.
- [4] S. Boyd, N. Parikh, E. Chu, B. Peleato, J. Eckstein, Distributed optimization and statistical learning via the alternating direction method of multipliers, Foundations and Trends in Machine Learning 3 (2011) 1–122.
- [5] H. Cardot, F. Ferraty, P. Sarda, Functional linear model, Statistics and Probability Letters 45 (1999) 11–22.
- [6] H. Cardot, F. Ferraty, P. Sarda, Spline estimators for the functional linear model, Statistica Sinica 13 (2003) 571–591.
- [7] G. Claeskens, K. Tatyana, D. O. Jean, Asymptotic properties of penalized spline estimators, Biometrika 96 (2009) 529–544.
- [8] J. Fan, R. Li, Variable selection via nonconcave penalized likelihood and its oracle properties, Journal of the American Statistical Association 96 (2001) 1348–1360.
- [9] Y. Fang, T. Fu, T. C.M. Lee, Functional mixture regression, Biostatistics 12 (2011) 341–53.
- [10] C. Garoni, C. Manni, F. Pelosi, S. Serra-Capizzano, H. Speleers, On the spectrum of stiffness matrices arising from isogeometric analysis, Numerische Mathematik 127 (2014) 751–799.
- [11] N. Hilgert, A. Mas, N. Verzelen, Minimax adaptive tests for the functional linear model, The Annals of Statistics 41 (2013) 838–869.
- [12] X. Hu, J. Huang, L. Liu, D. Sun, X. Zhao, Subgroup analysis in the heterogeneous cox model, Statistics in Medicine 40 (????) 739–757.
- [13] J. Hua, Y. Zhang, B. D. Foy, X. Mei, J. Shang, C. Feng, Competing pm2.5 and no2 holiday effects in the beijing area vary locally due to differences in residential coal burning and traffic patterns, Science of The Total Environment 750 (2021) 141575.
- [14] X. Lan, A. Qu, J. Zhou, Consistent model selection for marginal generalized additive model for correlated data, Journal of the American Statistical Association 105 (2010) 1518–1530.
- [15] T. Lyche, C. Manni, H. Speleers, Foundations of spline theory: B-splines, spline approximation, and hierarchical refinement, Foundations of Spline Theory: B-Splines, Spline Approximation, and Hierarchical Refinement, Springer, 2018, pp. 34–56.
- [16] S. Ma, J. Huang, A concave pairwise fusion approach to subgroup analysis, Journal of the American Statistical Association 112 (2017) 410–423.
- [17] S. Ma, Z. Zhang, J. Huang, M. Liu, Exploration of heterogeneous treatment effects via concave fusion, The International Journal of Biostatistics 16 (2020). Online.
- [18] C. Preda, G. Saporta, Clusterwise pls regression on a stochastic process, Computational Statistics and Data Analysis 48 (2005) 149–158.
- [19] J. O. Ramsay, B. W. Silverman, Applied Functional data analysis, Vol.77. Springer, New York, 2002.
- [20] J. O. Ramsay, B. W. Silverman, Functional data analysis, Springer, New York, 2005.
- [21] R. Tibshirani, M. Saunders, S. Rosset, J. Zhu, K. Knight, Sparsity and smoothness via the fused lasso, Journal of the Royal Statistical Society 67 (2005) 91–108.
- [22] H. Wang, B. Li, C. Leng, Shrinkage tuning parameter selection with a diverging number of parameters, Journal of the Royal Statistical Society: Series B (Statistical Methodology) 71 (2009) 671–683.
- [23] C. Zhang, Nearly unbiased variable selection under minimax concave penalty, The Annals of Statistics 38 (2010) 894–942.
- [24] S. Zhou, X. Shen, D. A. Wolfe, Local asymptotics for regression splines and confidence regions, The Annals of Statistics 26 (1998) 1760–1782.
- [25] X. Zhu, A. Qu, Cluster analysis of longitudinal profiles with subgroups, Electronic Journal of Statistics 12 (2018) 171–193.